ACTIVE POWER FILTER WITH CONSTANT SWITCHING FREQUENCY FOR REACTIVE POWER AND HARMONIC COMPENSATION

by

Shyam Sundar

EE
1996
M
SUN
ACT

DEPARTMENT OF ELECTRICAL ENGINEERING

INDIAN INSTITUTE OF TECHNOLOGY KANPUR

JANUARY, 1996

ACTIVE POWER FILTER WITH CONSTANT SWITCHING FREQUENCY FOR REACTIVE POWER AND HARMONIC COMPENSATION

A Thesis Submitted
in Partial Fulfillment of the Requirements
for the Degree of

MASTER OF TECHNOLOGY

By

Shyam Sundar

to the

DEPARTMENT OF ELECTRICAL ENGINEERING

INDIAN INSTITUTE OF TECHNOLOGY KANPUR

JANUARY, 1996

11 APR 1996/EE

No. A. 121283

EE-1996-M-SUN-ACT

A121 3

Certificate

It is certified that the work contained in the thesis entitled **ACTIVE POWER FILTER WITH CONSTANT SWITCHING FREQUENCY FOR REACTIVE POWER AND HARMONIC COMPENSATION** by *Shyam Sundar* has been carried out under our supervision and that this work has not been submitted elsewhere for a degree.

(Dr B.G. Fernandes)
Assistant Professor
Department of Electrical Engineering
Indian Institute of Technology
Kanpur-208016 India

(Dr S.C. Srivastava)
Professor
Department of Electrical Engineering
Indian Institute of Technology
Kanpur-208016 India

GRADUATE OFFICE
I.I.T. Kanpur.
Submitted on 23/1/96

dedicated to my Parents

Acknowledgement

It is with a deep sense of gratitude that I acknowledge the invaluable guidance received from Dr. S.C. Srivastava and Dr. B.G. Fernandes, both of whom have been a source of constant encouragement during this work.

I am thankful to Dr. S.S. Prabhu, Dr. Sachidanand, Dr. G.K. Dubey, Dr. R.K. Varma and Dr. A.Joshi who helped me to build the foundation for this work.

I am greatly indebted to my senior colleagues B. Das, S.K. Joshi, R.P. Gupta, S.N. Singh and K.N. Srivastava for their useful discussions in connection with this work.

Special thanks goes to my friends Desh Raj Singh, Alok Kumar Tyagi, P. Moghe, Hemant Agrwal and D.V. Raman without whom unfailing support and untiring help it would have been hard for me to bring out this thesis in the form it appears today.

Shyam Sundar

Abstract

The wide use of nonlinear loads controlled by converter/inverter has resulted in a number of undesirable effects such as increased reactive power demand and harmonic pollution in the operation of power system. This results in reduction of overall supply power factor. The active power filters are used for reducing harmonic content and reactive power demand from the source. In this thesis the performance of single phase and three phase active power filter with fixed switching frequency is analysed. The proposed active power filter uses a PWM voltage source inverter. It operates with almost constant switching frequency and can compensate the reactive power and the current harmonic components of nonlinear loads. The fixed switching frequency operation of the device is obtained using adaptive hysteresis band current controller. The reactive power compensation and harmonic reduction is done without analysing the load current. This results in simplified control system. The compensation is done in time domain in order to improve the response, instead of frequency domain correction. The performance of the active power filter compensating the various nonlinear loads is predicted by off line simulation studies. Results show that there is significant improvement in the supply power factor and harmonic content, there by reducing the burden on the power generator.

Contents

Chapter 1

Introduction

1.1 General

Traditionally, the major part of power is consumed by loads such as incandescent lighting, heating, and ac motors, which draw sinusoidal current when they are energized by sinusoidal voltage. However, this situation is rapidly changing as more products are being developed that condition the power through the use of power electronic devices. These power electronic devices are now able to process large amount of power, and due to their advantages such as increased efficiency and ease of control, have caused a dramatic increase in the number of power electronic loads in the system. Unfortunately, power electronic loads possess an inherent nonlinear characteristics, and therefore draw a distorted current from the supply. These distorted currents cause an increase in apparent power consumed. Non-sinusoidal supply currents also cause overheating in supply transformers and interfere with the neighbouring communication circuits.

To suppress the harmonics, passive shunt filters which are being used are tuned to the frequency of the harmonic to be reduced. These are also used for reactive power compensation or power factor improvement. Some of the benefits of power factor improvement and harmonic filtering are:

- reduced power loss,
- better utilization of generation, transmission, distribution and substation capacity,
- reduced voltage drop and improved voltage regulation,
- elimination of interference with communication lines,
- improved quality of electric energy at the user's end,
- increased life span of the equipments.

The shunt passive filters exhibit lower impedance at a tuned harmonic frequency than the source impedance, so that reduced harmonic currents flow into the source. However, the filtering characteristics of shunt passive filter are determined by the impedance ratio of the source and the shunt passive filter. Therefore, shunt passive filters have the following problems which discourage their applications:

(i) The source impedance, which is not accurately known and varies with the system configuration.

(ii) The shunt passive filter acts as a sink to the harmonic current flowing from the source. In the worst case, the shunt passive filter will resonate(series) with the source impedance. This results in excessive harmonic currents flowing into the passive filter.

(iii) At a specific frequency, parallel resonance might occur between the source and the shunt passive filter, which is known as harmonic amplification.

(iv) They are generally tuned to remove specific frequency components and therefore not a completely satisfactory solution when the harmonic composition of the distorted waveform changes.

(v) As both the harmonic and the fundamental current components flow into the filter, the capacity of the filter must be rated by taking into account both currents.

(vi) When the harmonic current components increases, the filter can be overloaded.

Active power filters have been suggested to compensate for reactive power, negative-sequence current and harmonics in industrial power systems. Active power filters are used to correct network distortions caused by power electronic loads by injecting equal but opposite distortion at carefully selected points in a network.

In this thesis an indepth study has been carried out for development of both single phase and three phase active filters.

1.2 Motivation

The main motivation of the work is to study the behavior of single phase and three phase active power filters which are capable of supplying reactive power to the load and generating the harmonics so that the current drawn from the supply is sinusoidal and in phase with the voltage.

The active power filter consists of

(a) power converter made of IGBT switches,

(b) dc capacitor, and

(c) inductor.

The active filter is controlled through two control loops:

1. The inner current regulation loop,

2. The outer voltage control loop, which regulates the average voltage on the dc capacitor. This loop is responsible for correctly setting the magnitude of the reference phase currents.

In order to maintain the switching frequency constant, adaptive hysteresis band

controller is used. Depending upon the magnitude of current, supply voltage, capacitor voltage and inductance, the controller calculates the width of the band so that the switching frequency is maintained around 6kHz. Depending upon the error in the dc link voltage the outer voltage control loop generates the reference current, without sensing the load current. It is assumed that the active power filter is capable of supplying the entire reactive power demand of the load.

1.3 Literature Review

With the development of high power self commutated switches(GTO 1-kHz,4500V, 3000A; BJT 1200V,800A,10kHz; IGBT 20-kHz,1200V, 400A [24]) the interest has been increased in the study of active power line conditioners for reactive and harmonic compensation. At present, the purpose of shunt active conditioners is to compensate for reactive power, negative sequence current and harmonics.

There are many papers available on shunt passive filters and active power filters. But in this thesis the review is limited to some key papers and recent publications in this field [4, 7, 12, 20, 25, 29, 32, 35, 40, 43, 44].

The active power filters use either voltage source inverter(VSI) [4, 25, 29, 32, 35, 40, 43, 44] or current source inverter(CSI) [7, 12, 20] as power converter. Voltage source converter type of active power filters can readily expanded in parallel to increase their combined rating [4]. Their combined switching rate can be increased if they are carefully controlled so that their individual switching instants do not coincide. Therefore, higher-order harmonics can be eliminated by using parallel voltage type converters without increasing individual converter switching frequency. Also, voltage-type converters are lighter, more efficient and less expensive than current-type converters [28]. However, main drawback of voltage type converter is the increased complexity of control system when they are connected in parallel.

Akagi et al [4] described an active filter using multiple voltage source inverters and a time-delay PWM switching strategy. A followup paper [13] deals with the

control circuit, which is based on instantaneous reactive power, and performance for improved transient response of the active filter.

Duke and Round [25] have used a high-frequency VSI and a time-delay switching strategy for a single phase active power filter. Unlike fixed frequency PWM technique, the switching strategy produces an inverter output current which is asynchronous. A synthetic sinusoid is used to determine the distortion component of the load current. Capacitor voltage controller is not used. They claim that the inverter dc bus voltage can be controlled by manipulating the amplitude of the reference sinusoid. Zero-crossing detector and phase-locked loop have been used to determine the fundamental load current. An intelligent controller is suggested to improve the performance of active power filter at the optimal operating point under varying load conditions. It has been further improved by Round and Duke [35] by using simplex optimization technique to improve active filter performance. The basis for this optimization is the development of a saving function which takes into account the efficiency of the active filter, the cost of energy, and the supply current distortion. The goal is to maximize the monetary saving and operating efficiency while minimizing supply current distortion.

Malesani et al [20] proposed an active power filter which includes both inductive and capacitive energy storage circuits together with a half-controlled bridge to interface them. The whole system can be considered as an active power filter with hybrid energy storage. Current source converters use inductive storage and voltage source converters use capacitive storage. This scheme is aimed to take the advantages of voltage source or capacitive storage (efficient, smaller and less expensive) and current source or inductive storage (accurate current control, reliable and fault-tolerant) circuits. However, the control system is very complex.

Torrey and Zamel [44] suggested sliding mode control for single phase active power filter which is further extended by Saetieo et al [43] for three phase active filters. Their study is limited to steady state analysis.

1.4 Thesis Organization

Chapter 1 gives an introduction to this thesis explaining the main motivation of the work and a critical review of control schemes existing in the literature.

Detailed analysis of a single phase active power filter and off line simulation studies to predict its performance during steady state and transient conditions are discussed in chapter 2. Expression for the variable hysteresis band to maintain the constant switching frequency of the inverter is also derived in this chapter.

Performance prediction during steady state and transient condition of the 3-phase active power filter compensating non-linear unbalanced loads is dealt in chapter 3.

Chapter 4 summarizes the contribution of this work and gives suggestions for further work in this direction.

Chapter 2

Single-Phase Active Power Filter

2.1 Introduction

Converter/inverter driven loads are increasingly being used in the industry. These loads draw non-sinusoidal current from the supply. This results in the reduction in overall supply power factor and increased harmonic content. However. due to recent advances in semiconductor technology, it is now possible to efficiently use active filters [25, 29, 44] to remove these harmonics which overcome many disadvantages of traditional passive filters.

Torrey et al [44] described a single phase active power filter based on a single-phase converter with four switches. The controller is based on sliding mode control law. Duke et al [25] described a single phase active power filter using a high-frequency VSI and a time-delay switching strategy. They used a signal processing unit for reference current generation. A follow-up paper [35] describes the real time optimization of active filter's performance using simplex optimization technique and is implemented using TMS320C30 DSP. Enjeti et al [29] have proposed single phase active filter to cancel neutral current harmonics in three-phase four-wire electric distribution systems.

This chapter deals with the detailed analysis and simulation studies of a single

phase active power filter. The single phase active power filter has following features:

(i) It compensates the reactive and harmonic part of load current without calculating the load current components(real or reactive or harmonic), thus simplifying the control system.

(ii) Adaptive hysteresis band current control scheme [24] is used to determine the width of the hysteresis band. The width of band is calculated in such a way that the switching frequency of the device remains almost constant at 6kHz.

(iii) The current compensation is used in time domain in order to improve the response, instead of frequency domain correction [15].

Simulation results are obtained to show typical waveforms and prove the capability and the performance of the proposed filter.

2.2 The Converter Model

The power circuit of the system is shown in Fig.2.1. The active filter consists of a capacitor, an inductor and four controllable switches with antiparallel diodes. The switches S_1, S_2, S_3, and S_4 are operated in such a way that the total current drawn by the filter and the nonlinear load is of the correct magnitude and of the same shape as that of the ac source voltage v_s.

The Kirchhoff's Voltage Law for the above circuit can be written as–

$$v_s = L\frac{di_L}{dt} + R.i_L + s.v_c \tag{2.1}$$

or

$$\frac{di_L}{dt} = \left(\frac{v_s - R.i_L - s.v_c}{L}\right) \tag{2.2}$$

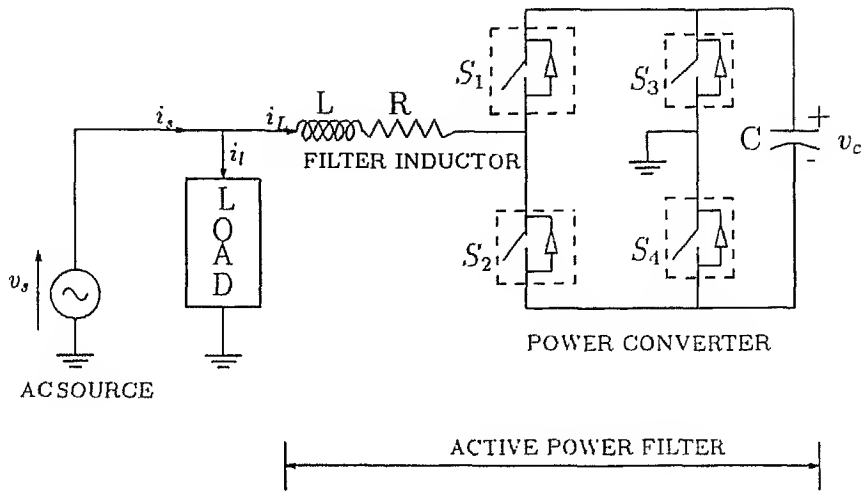

Figure 2.1: Single-phase active power filter configuration

where

v_s = ac source voltage
$= Vm \cdot \sin(\omega t)$
L = synchronous link inductance or filter inductance
R = resistance of the inductor and the equivalent resistance of the switching devices.
i_L = compensator current or filter inductor current
v_c = voltage across the capacitor
s = switching function, which is defined as follows:

$$= \begin{cases} 1 & \text{if switches } S_1 \text{ and } S_4 \text{ conduct} \\ -1 & \text{if switches } S_2 \text{ and } S_3 \text{ conduct} \\ 0 & \text{if switches } S_1, S_3 \text{ or } S_2, S_4 \text{ conduct} \end{cases} \tag{2.3}$$

It is evident from equations (2.2) and (2.3) that the compensator current(i_L) can have any shape. This can be achieved by controlling the switches. In order to decrease the current i_L , $s = 1$ and for increasing the current, $s = -1$. Depending upon the sign of v_s, the current i_L will increase or decrease when $s = 0$.

The capacitor voltage v_c can be written as-

$$C\frac{dv_c}{dt} = s \cdot i_L$$

$$or$$

$$\frac{dv_c}{dt} = \frac{s.i_L}{C} \tag{2.4}$$

The equations (2.2) , (2.3) and (2.4) give the mathematical model of the converter. In the matrix form the state equations can be written as:

$$\frac{d}{dt}\begin{bmatrix} i_L \\ v_c \end{bmatrix} = \begin{bmatrix} \frac{-R}{L} & \frac{-s}{L} \\ \frac{s}{C} & 0 \end{bmatrix}\begin{bmatrix} i_L \\ v_c \end{bmatrix} + \begin{bmatrix} \frac{v_s}{L} \\ 0 \end{bmatrix} \tag{2.5}$$

2.3 The Control Law

The purpose of the active power filter is to force the source current to be of the same shape as v_s and in phase with v_s. By KCL from fig.2.1, the source current i_s is given by -

$$i_s = i_L + i_l \tag{2.6}$$

where i_l = load current,

From equation (2.6) :

$$\frac{di_s}{dt} = \frac{di_L}{dt} + \frac{di_l}{dt} \tag{2.7}$$

Using equation (2.2), (2.7) can be written as:

$$\frac{di_s}{dt} = \left(\frac{v_s - R \cdot i_L - s \cdot v_c + L \cdot \frac{di_l}{dt}}{L}\right) \tag{2.8}$$

We have no control over any other variable in equation (2.8) except on the switching function s. Hence for proper control of the source current i_s

$$|v_c| > |v_s|_{max} + |L \cdot \frac{di_l}{dt}|_{max} + |R \cdot i_L|_{max} \tag{2.9}$$

or by neglecting R ,

$$|v_c| > |v_s|_{max} + |L \cdot \frac{di_l}{dt}|_{max} \tag{2.10}$$

If $i_s > i_s^*$, S_1 and S_4 are turned ON($s = 1$). The rate of change of i_s will be negative and hence current i_s will decrease. And if $i_s < i_s^*$, S_2 and S_3 are turned ON($s = -1$). The rate of change of i_s will be positive and the current i_s will increase, where i_s^* is the reference source current. Therefore, the control law can be summarized as:

current status	*switches to be ON*
$i_s > i_s^*$	S_1 & S_4
$i_s < i_s^*$	S_2 & S_3

To ensure the controllability of current i_s , inequality (2.10) must always be satisfied for all possible values of load current i_l.

2.4 The Reference Current Generation And The Capacitor Voltage Control Loop

For proper operation of the power converter as active power filter the capacitor voltage must always be higher than the peak of ac source voltage(V_m). This limit on v_c is said as the loss of control limit [9] and is confirmed by equation (2.2). This will ensure the diodes be normally reverse-biased and the current i_L can be maintained at any required value by turning the switches ON or OFF. Also, the capacitor voltage must be sufficiently high so that the modulator is capable of tracking the reference current waveform. For this, the inequality (2.10) must be satisfied and hence the capacitor voltage control.

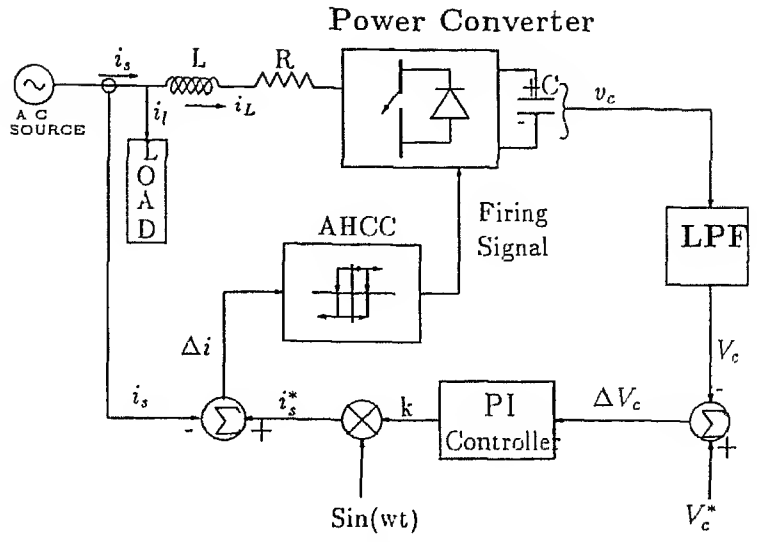

Figure 2.2: Control block diagram

The block diagram of capacitor voltage control and reference current generation loop is shown in Fig.2.2.

The voltage control loop generates the magnitude of the source current reference(k) through a proportional-integral (PI) controller which regulates the average capacitor voltage (V_c). The average capacitor voltage is obtained by using a low pass filter whose transfer function is given by:

$$G_{LPF}(s) = \frac{G}{1 + \frac{2\cdot\xi}{\omega_0}\cdot s + \frac{s}{\omega_0}^2} \tag{2.11}$$

where

G = gain of the filter;

ξ = damping ratio;

$\omega = 2 \cdot \pi \cdot f_0$

f_0 = characteristic frequency or cut off frequency of the filter.

Through trial and error it was found that G = 1.0 , ξ = 1.0 , and f_0 = 5 to 10 Hz which gives the better results for this scheme.

The output of the PI controller is the amplitude (k) of the current which is used to derive the reference source current waveform. The reference waveform for the ac source current i_s^* is obtained by multiplying k with $\frac{v_s}{V_m}$ or sin($\omega \cdot$ t). In other words by synchronising the output of PI controller with the ac source voltage the reference current waveform is obtained. Thus the reference current is of the same shape as the ac source voltage and in phase with it. This current can be actively generated by the current control law which is discussed in the previous section.

The stability of the active filter is evaluated by its ability to keep the dc voltage of the capacitor close to the reference value. The capacitor voltage control loop assumes that the active power supplied by the source is the sum of power drawn by the load and the losses in the inverter. During sudden increase in load power demand, capacitor voltage will decrease because the stored energy in the capacitor will supply the power to the load. This results in increase in the capacitor error voltage $\Delta V_c (= V_c^* - V_c)$ and the magnitude of reference current. This increase in current recharges the capacitor to the reference value. In the case of decreased load demand , the reverse action will take place. The decrease in the capacitor voltage must not be below controllability limit($V_c > V_m$); hence the larger capacitor should be used.

2.5 Current Control Strategies

The following are the main current control strategies reported in the literature ,

- Hysteresis Current Control [3,6,9,10,25,41] ;
- Current Control with triangularization of error [18,27,40,45] ;
- Predicted Current Control [11,17,30]
- Adaptive hysteresis band control [2,14,26].

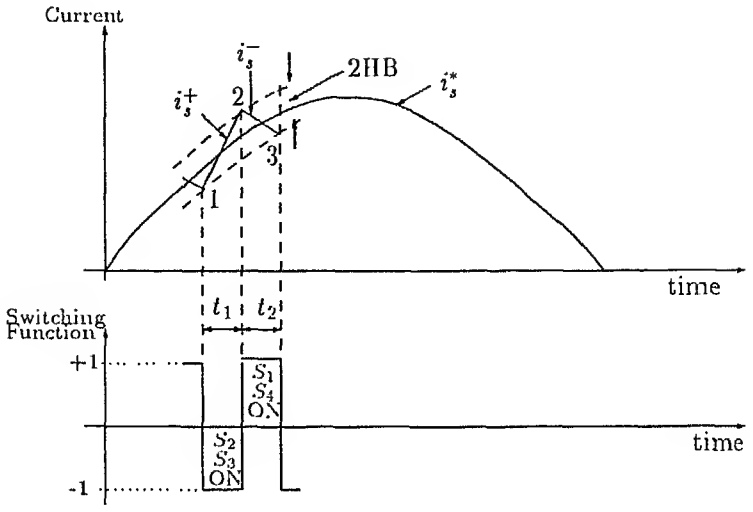

Figure 2.3: Current and switching function for adaptive hysteresis-band current control

The hysteresis current control strategy is the simplest one, but its major drawback is that the average switching frequency varies with the load current. The remaining control strategies operate on constant switching frequency. However, in second and third schemes, the stability of operation of the current loop is ensured only if correct system parameters and load current values are known. In adaptive hysteresis band control the switching frequency is maintained constant by varying the hysteresis band over the cycle. Since it is easy to implement and has stable operation with lesser dependency on the load current, this scheme is used in the present work.

2.5.1 Derivation of Expresion for Adaptive Hysteresis Band

Fig.2.3 shows the current and switching signal waveforms for current control. The actual source current tends to cross the lower hysteresis band at point-1, where the switches S_2 and S_3 are switched ON. The linearly rising current (i_s^+) then touches the upper band at point-2, where the switches S_1 and S_4 are turned ON. With reference

to equation(2.8), the respective equations for switching intervals t_1 and t_2 can be written as:

$$\frac{di_s^+}{dt} = \frac{1}{L} \cdot (v_s - R \cdot i_L + v_c) + \frac{di_l}{dt} \tag{2.12}$$

and

$$\frac{di_s^-}{dt} = \frac{1}{L} \cdot (v_s - R \cdot i_L - v_c) + \frac{di_l}{dt} \tag{2.13}$$

where i_s^+ and i_s^- are the rising and falling currents respectively.

From the geometry of the fig.2.3, we can write

$$\left(\frac{di_s^+}{dt} - \frac{di_s^*}{dt}\right) \cdot t_1 = 2 \cdot HB \tag{2.14}$$

and

$$\left(\frac{di_s^-}{dt} - \frac{di_s^*}{dt}\right) \cdot t_2 = -2 \cdot HB \tag{2.15}$$

also

$$t_1 + t_2 = T_s = \frac{1}{f_s} \tag{2.16}$$

where f_s is the switching frequency and HB is the hysteresis band.

From equations (2.12) to (2.16), it can be shown that:

$$HB = \left(\frac{0.25 v_c}{f_s L}\right) \cdot \left(1 - \left(\frac{v_s - R \cdot i_L + L\frac{di_l}{dt} - L\frac{di_s^*}{dt}}{v_c}\right)^2\right) \tag{2.17}$$

where i_s^* is the reference source current which is of the form

$$i_s^* = k \cdot \sin(\omega t) \tag{2.18}$$

hence

$$\frac{di_s^*}{dt} = k \cdot \omega \cdot \cos(\omega t) \tag{2.19}$$

The maximum switching frequency for a specified hysteresis band is:

Table 2.1: Hysteresis Current Control Rule

current error	*switches to be ON*
$\Delta i_s > HB$	S_2 & S_3
$\Delta i_s < -HB$	S_1 & S_4
$-HB \leq \Delta i_s \leq HB$	No change

$$f_s^{max} = \frac{0.25 v_c}{HB.L} \tag{2.20}$$

Equation(2.17) shows that the hysteresis band is a function of switching frequency(f_s). source voltage(v_s), and the slope of load current(i_l) and the source reference current(i_s^*). From equation(2.17) it can be written as:

$$f_s = \left(\frac{0.25 v_c}{HB \cdot L}\right) \cdot \left(1 - \left(\frac{v_s - R \cdot i_L + L\frac{di_l}{dt} - L\frac{di_s^*}{dt}}{v_c}\right)^2\right) \tag{2.21}$$

Equation(2.21) indicates that for a hysteresis band. the switching frequency will vary with load current. Also the switching frequency increases with v_c. Equation(2.17) shows that the hysteresis band can be modulated as a function of v_c and v_s, and the slope of currents i_l and i_s, so that the switching frequency remains almost constant. This will improve the converter performance substantialy.

The adaptive hysteresis current control strategy is shown in Table 2.1, where $\Delta i_s = i_s^* - i_s$.

2.6 Performance Analysis/Calculation

The performance of the active power filter can be evaluated by its efficiency, power factor of the ac source current and the total harmonic distortion(THD) of the source current. The total harmonic distortion is defined as:

$$THD(\%) = \left(\frac{\sqrt{\sum_{h=2}^{\infty}(I_{sh})^2}}{I_{s1}}\right) * 100 \tag{2.22}$$

where I_{s1} is the fundamental component and I_{sh} is the h^{th} harmonic of the source current. The power factor(pf) is given by:

$$pf = \mu \cdot cos(\phi_{s1}) \tag{2.23}$$

where ϕ_{s1} is the phase difference between the source voltage(v_s) and the fundamental source current(i_{s1}). $\cos(\phi_{s1})$ is called the displacement factor of the current; and μ is the distortion factor which is defined as:

$$\begin{aligned} \mu &= \frac{I_{s1}}{I_s} \\ &= \sqrt{\frac{1}{1+(THD)^2}} \end{aligned} \tag{2.24}$$

where I_s is the RMS value of the source current.

The efficiency(η) of the compensator is defined as:

$$\begin{aligned} \eta &= \left(\frac{P_{Load}}{P_{comp}+P_{Load}}\right) \\ &= \left(\frac{P_{Load}}{P_{Source}}\right) \\ &= \left(\frac{V_s I_{l1} cos(\phi_{l1})}{V_s I_{s1} cos(\phi_{s1}}\right) \\ &= \left(\frac{I_{l1}}{I_{s1}}.\right)\left(\frac{cos(\phi_{l1})}{cos(\phi_{s1})}\right) \end{aligned} \tag{2.25}$$

where ϕ_{l1} and ϕ_{s1} are the phase angle of fundamental load current(I_{l1}) and fundamental source current(I_{s1}) respectively, P_{load} is the power supplied by the source to the load and P_{comp} is the power supplied by the source to the compensator.

2.7 Power Circuit Design

The active filter power circuit is shown in fig.2.1. Active power filter consists of a capacitor(C), an inductor(L) and four controllable switches. Since switches must

support the unidirectional voltage and bidirectional current, GTO or transistor or IGBT with antiparallel diode is needed to implement each switch.

The current that is flowing in each switch is the maximum inductor current(i_L), and is given by:

$$i_L = i_s - i_l \tag{2.26}$$

where

$$i_s = \sqrt{2}\frac{P_{loads}}{V_{rms}} \cdot sin(\omega t) \tag{2.27}$$

The voltage which the devices must withstand is the maximum voltage across the capacitor. The capacitor voltage can be determined by equating the instantaneous power. That is, the part of the power delivered to the active filter at any instant is stored in the inductor(L) & capacitor(C), and the remaining power is dissipated in the resistor(R).

$$\int_0^t v_s \cdot i_L dt = \frac{1}{2}L(i_L)^2 + \frac{1}{2}C(v_c^2 - V_0^2) + R(i_L)^2 \tag{2.28}$$

or

$$v_c = \sqrt{V_0^2 + \frac{2}{C}\left(\int_0^t v_s \cdot i_L dt - \frac{1}{2}L(i_L)^2 - R(i_L)^2\right)} \tag{2.29}$$

From equation(2.29), it can be shown that:

$$C = \left(\frac{\frac{2}{V_0^2}\left(\int_0^t v_s i_L dt - \frac{1}{2}L(i_L)^2 - R(i_L)^2\right)}{\left(\frac{\Delta V}{V_0} + 1\right)^2 - 1}\right) \tag{2.30}$$

where $\Delta V = v_c - V_0$, V_0 is the capacitor voltage at $t = 0$.

For small ΔV:

$$C = \frac{1}{\Delta V \cdot V_0}\left(\int_0^t v_s i_L dt - \frac{1}{2}L(i_L)^2 - R(i_L)^2\right) \tag{2.31}$$

The required capacitor size for an acceptable voltage ripple can be determined using equation(2.31).

The selection of the inductance(L) value is based on equations(2.8) and (2.20). From equation(2.8), the ability to track the desired source current improves as the filter inductance is made smaller. Therefore as the value of the inductor decreases, the switching frequency of the devices increases. However, the ripple in the source current should be maintained to an acceptable value. Hence the value of the inductor should be determined from equation(2.20) to keep the current ripple and switching frequency to an acceptable value.

2.8 Simulation Results

The performance of the proposed active power filter and its control systems for reactive power support and harmonic cancelation has been studied for two types of non-linear loads through digital simulation. The simulation has been carried out using the electromagnatic transient simulation package PSCAD/$EMTDC^{TM}$ [46]. It is found that the performance of the proposed scheme is satisfactory for the types of loads considered. The details of the results are given below:

2.8.1 Case-1

The complete circuit used for simulation is shown in fig 2.4. The parameters of the active filter are $f_s = 6kHz, L = 20mH, C = 2000\mu F, V_c^* = 550V, K_p = 0.1, K_i = 1.0$.

The load consists of:

(i) a single phase diode bridge rectifier with dc side filter capacitor and resistive load,

(ii) a resistive load fed by a pair of antiparallel thyristors.

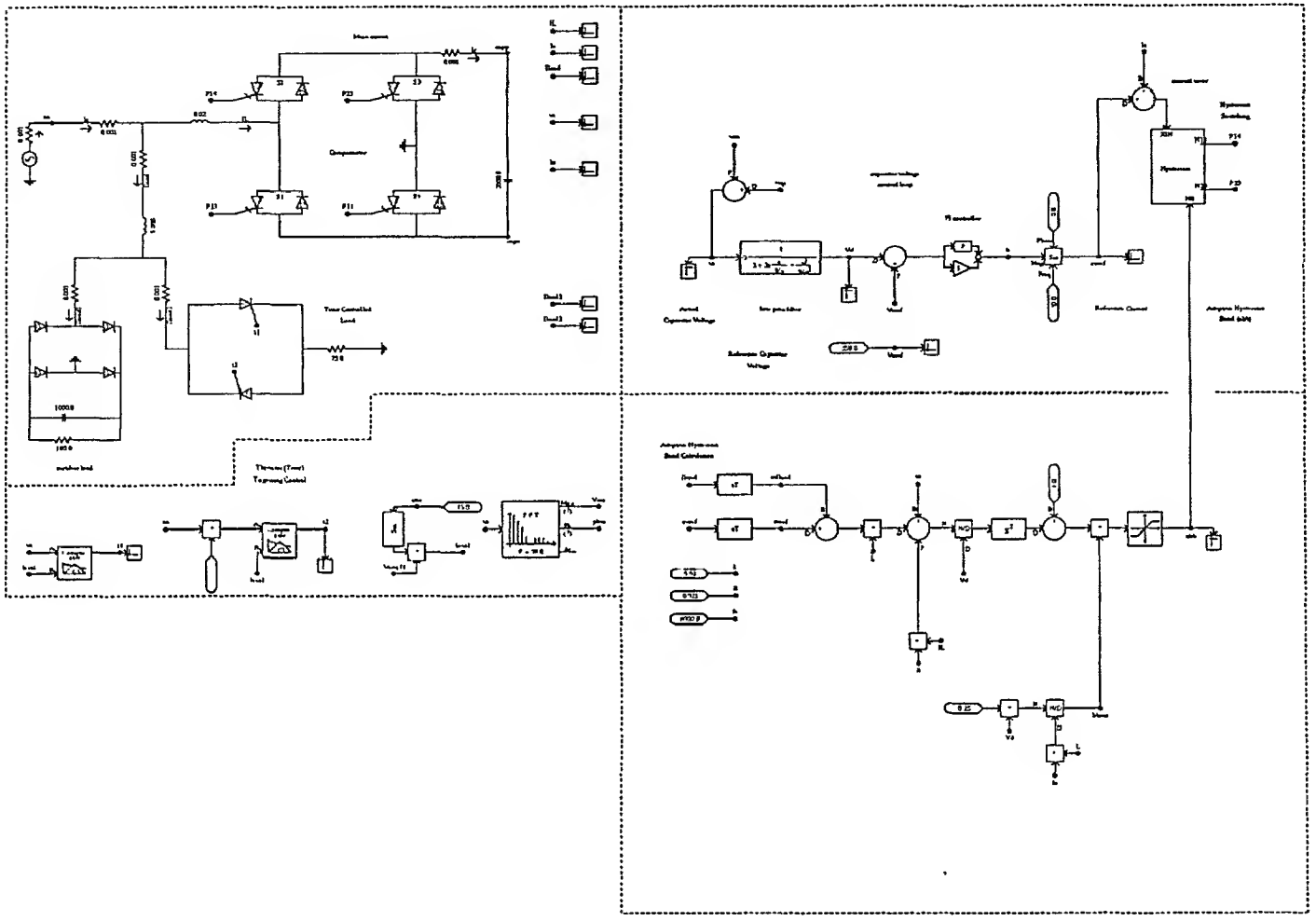

Figure 2.4: Block diagram for case-1

FIGURE 2.4(a) BLOCK DIAGRAM FOR CASE-1

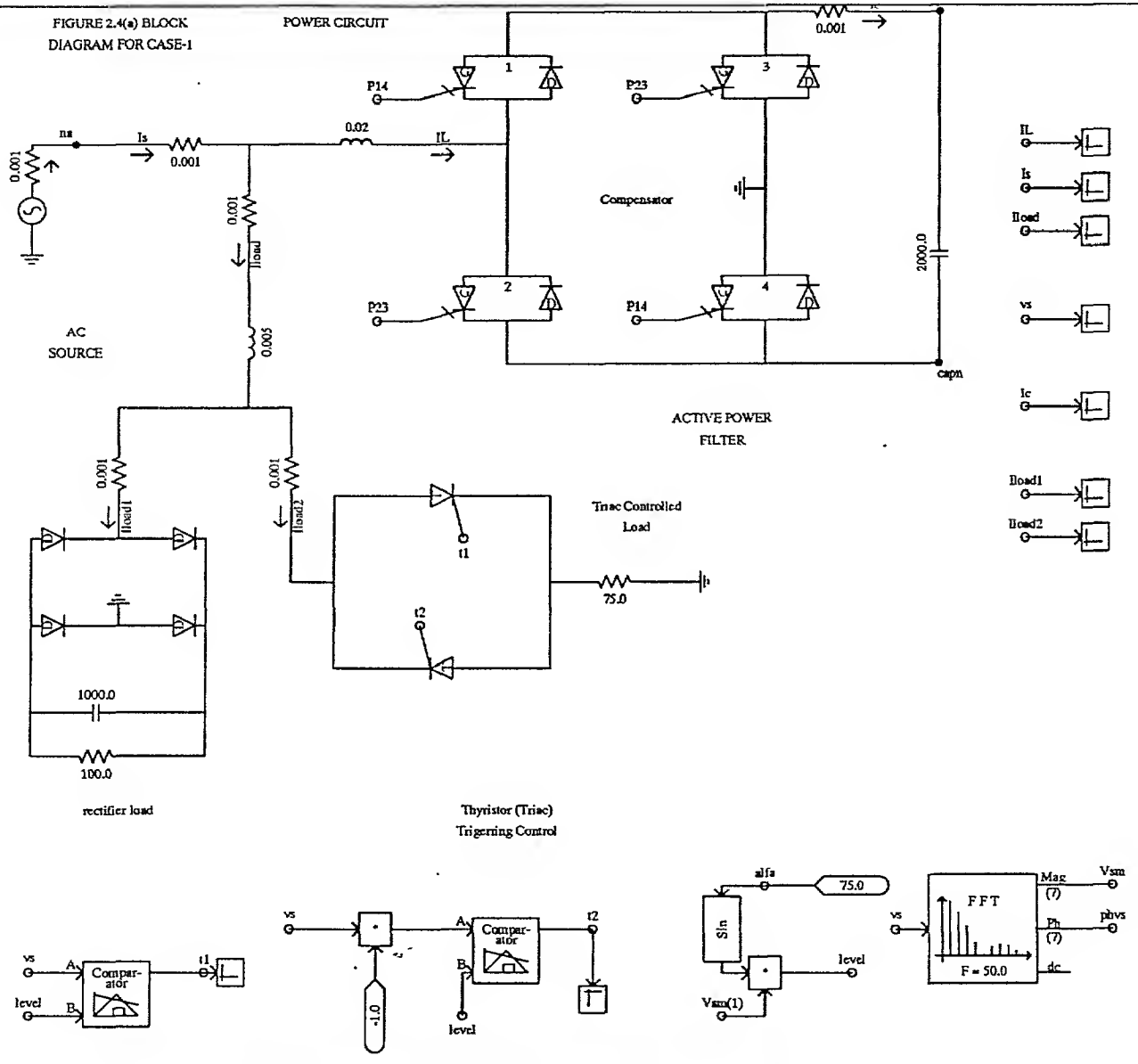

FIGURE 2.4
DIAGRAM

IIT Kanpur, INDIA *1-Phase*	Created: Last Modified: Printed On:	November 14, 1995 (shym) January 31, 1996 (shym) January 31, 1996 (shym)	*SS 1*

FIGURE 2.4(b) BLOCK DIAGRAM FOR CASE-1 CONTROL CIRCUIT

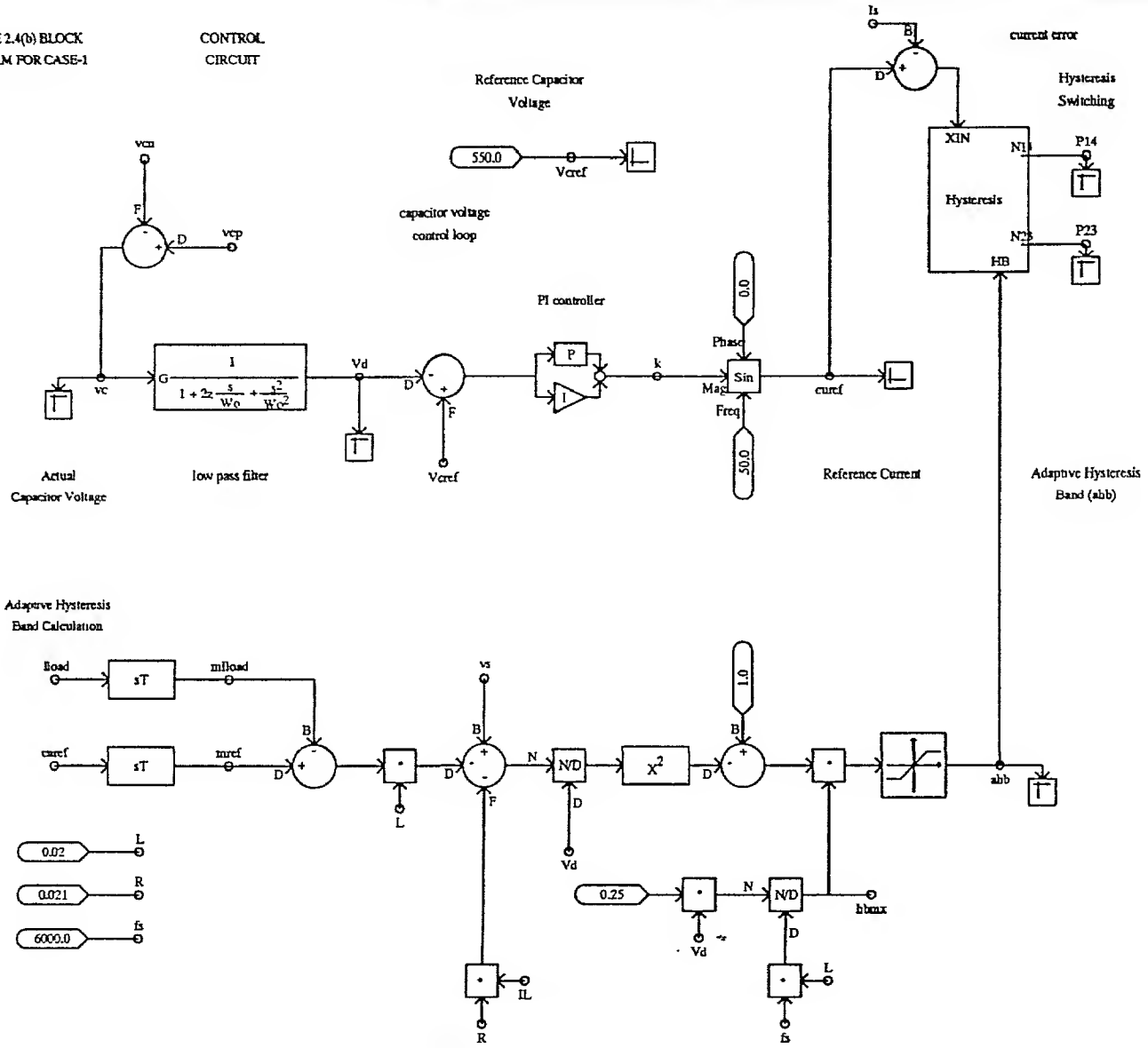

IIT Kanpur, INDIA *1-Phase*	Created: Last Modified: Printed On:	November 14, 1995 (shym) January 31, 1996 (shym) January 31, 1996 (shym)	*SS 1* Page 2 of 2

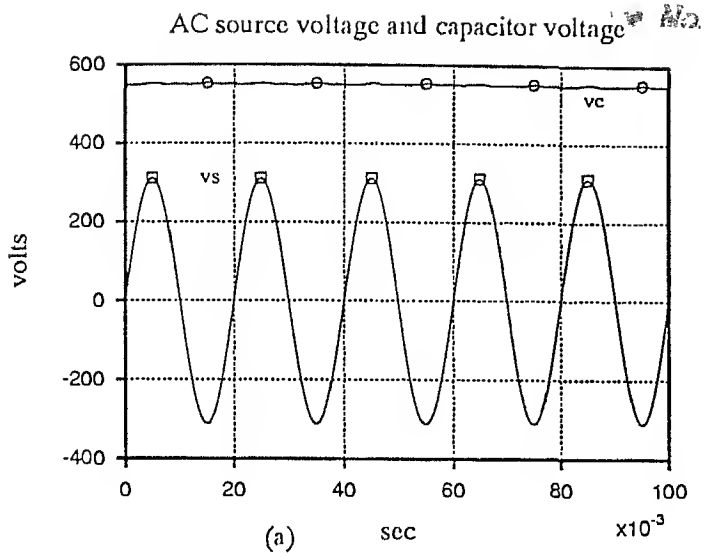
AC source voltage and capacitor voltage
volts
vc
vs
600
400
200
0
-200
-400
0
20
40
60
80
100
x10^-3
sec
(a)

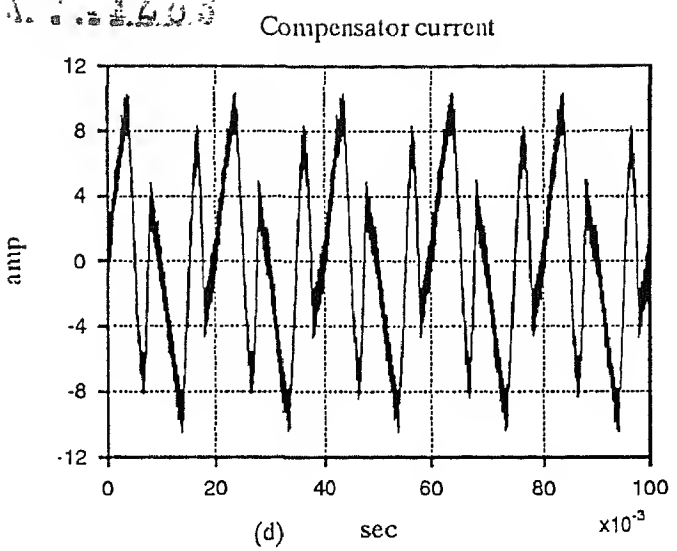
Compensator current
amp
12
8
4
0
-4
-8
-12
0
20
40
60
80
100
x10^-3
sec
(d)

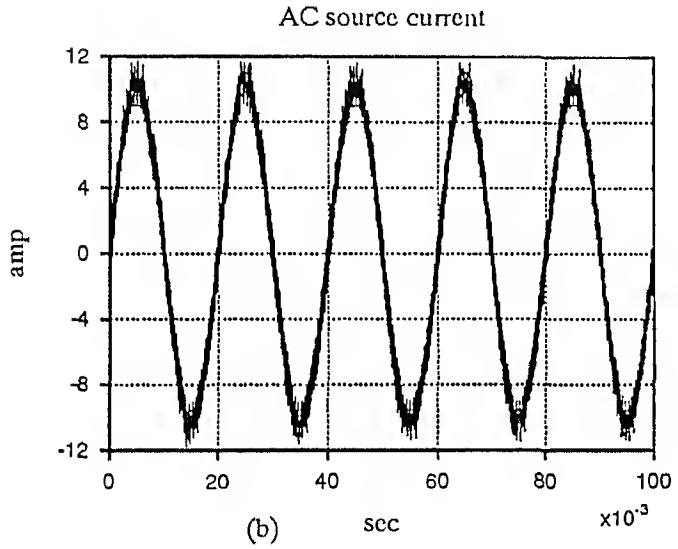
AC source current
amp
12
8
4
0
-4
-8
-12
0
20
40
60
80
100
x10^-3
sec
(b)

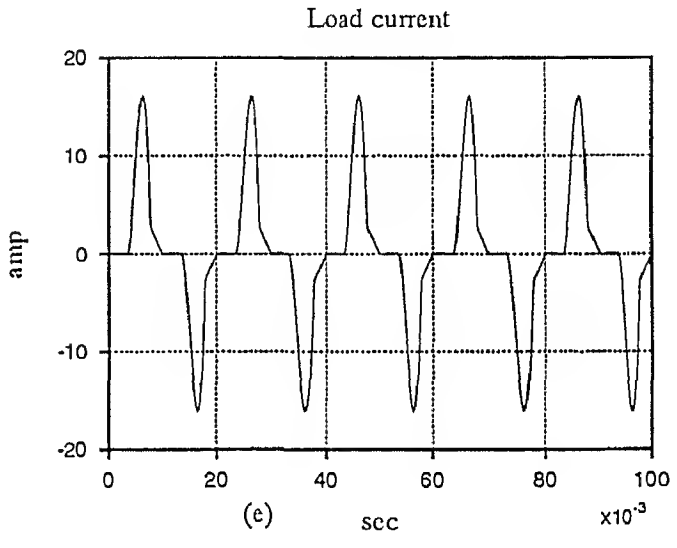
Load current
amp
20
10
0
-10
-20
0
20
40
60
80
100
x10^-3
sec
(e)

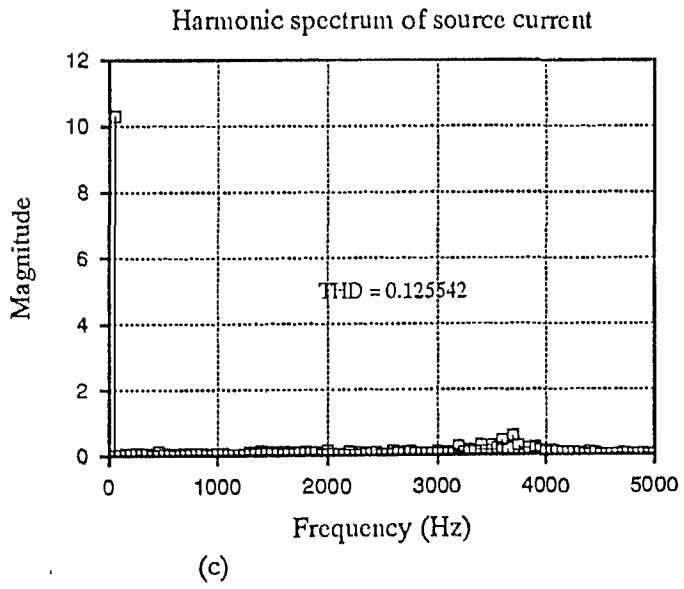
Harmonic spectrum of source current
Magnitude
THD = 0.125542
12
10
8
6
4
2
0
0
1000
2000
3000
4000
5000
Frequency (Hz)
(c)

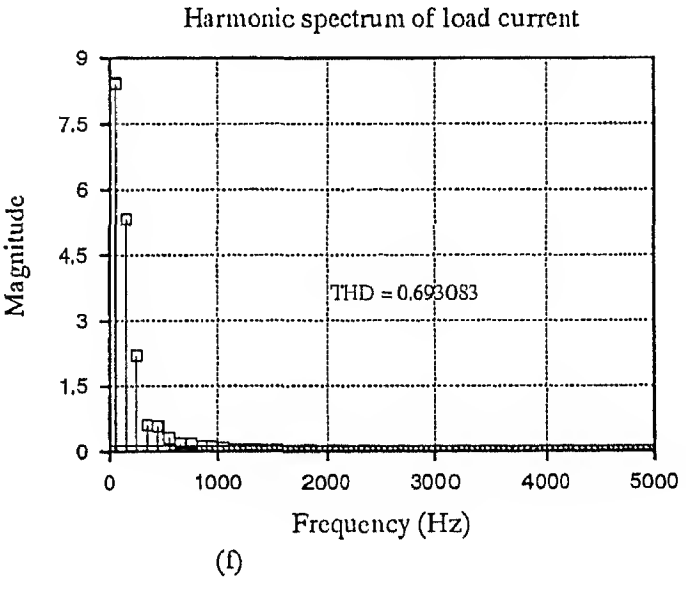
Harmonic spectrum of load current
Magnitude
THD = 0.693083
9
7.5
6
4.5
3
1.5
0
0
1000
2000
3000
4000
5000
Frequency (Hz)
(f)

The current drawn by the load and its harmonic spectrum are shown in fig.2.5(e) and fig.2.5(f) respectively. The THD of the load current and the load power factor are found to be 69.3% and 0.7512 respectively. Fig.2.5(b) and fig.2.5(c) show the source current waveform and its harmonic spectrum respectively. The THD of the source current and power factor are found to be 12.6% and 0.9922 respectively. This improvement in THD and power factor is due to the active power filter which generates harmonics to compensate with those drawn by the load. The current drawn by the compensator is shown in fig.2.5(d) and the capacitor voltage build up is shown in fig.2.8(a).

2.8.2 Case-2

The simulated results for the block diagram shown in fig.2.6, in which the active filter compensates the rectifier load is given in fig.2.7. The parameters of the active filter are: $f_s = 6kHz, L = 20mH, C = 2000\mu F, V_c^* = 650V, K_p = 0.1, K_i = 1.0$. The THD of the load current and the load power factor are found to be 33.2% and 0.7373 respectively. Whereas the THD of the supply current and the supply power factor are found to be 7.2% and 0.9974 respectively. The corresponding compensator current and the capacitor voltage build up are shown in fig.2.7(d) and fig.2.8(b) respectively.

2.8.3 Performance of the Filter During Transient Condition

Fig.2.9 shows the simulated current and capacitor voltage waveforms during transient conditions. Initially the active filter was compensating a bridge rectifier load whose trigger angle was maintained at 45 deg. At $t = 1$ sec. the trigger angle is changed to zero degree which results in increase in load current. Initially this increase in load current is supplied by the capacitor. As a result the capacitor voltage falls. The PI controller generates higher value of reference current. This increase in the reference source current will maintain the capacitor voltage to its original value. It is also evident from the fig.2.9(a) and fig.2.9(c) that the source current is sinusoidal and in phase with the voltage during transient condition.

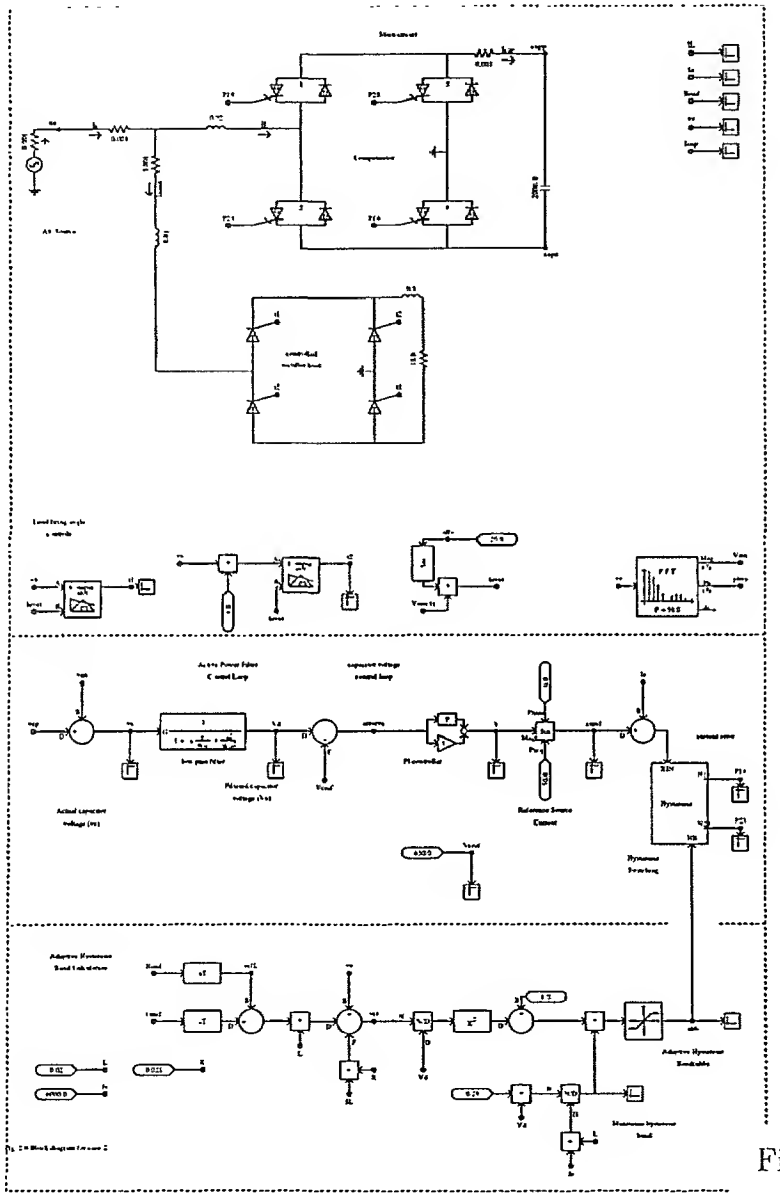

Figure 2.6: Block diagram for case-2

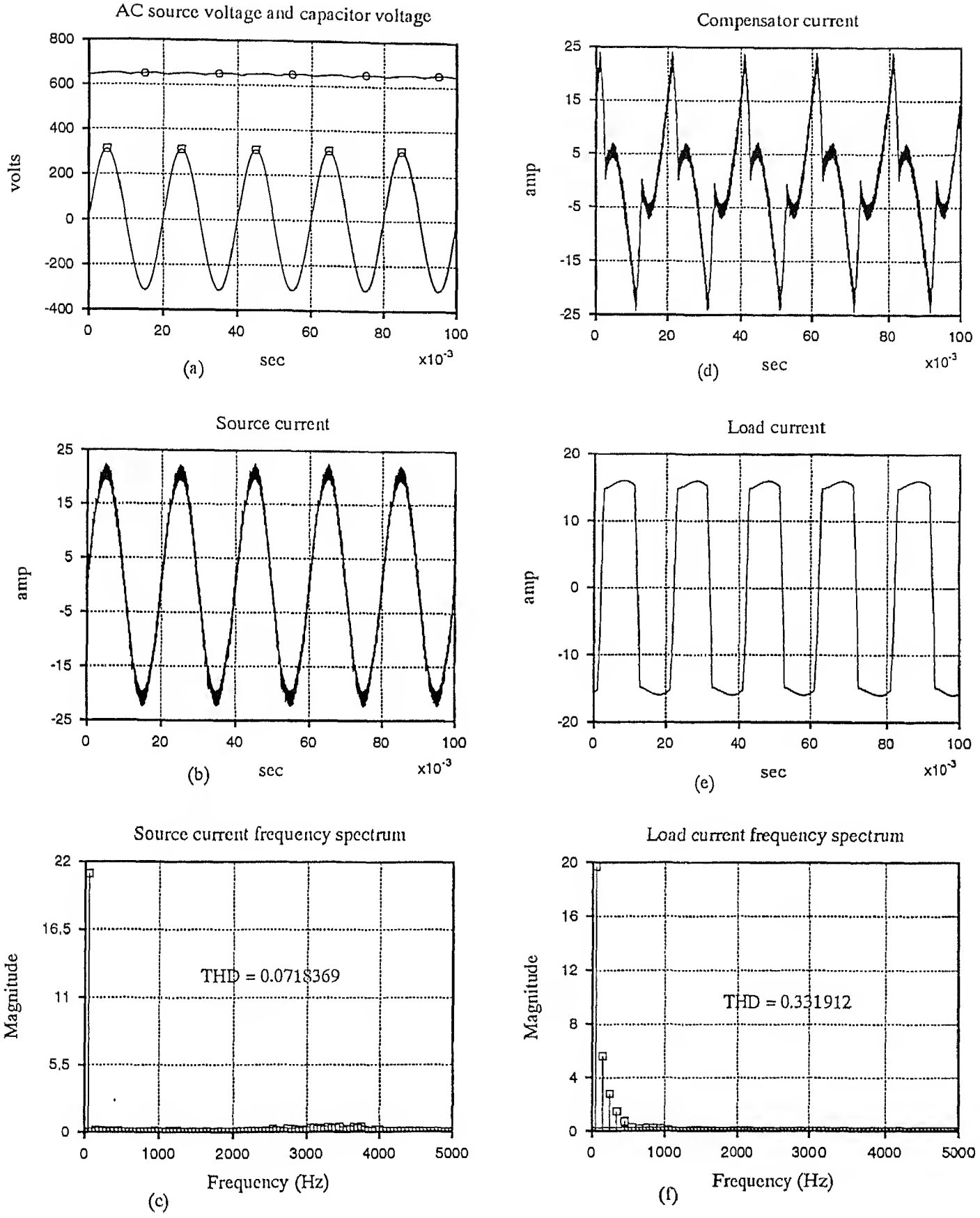

Fig.2.7 Simulated results for rectifier load (case-2)

(a) Capacitor voltage (case-1)

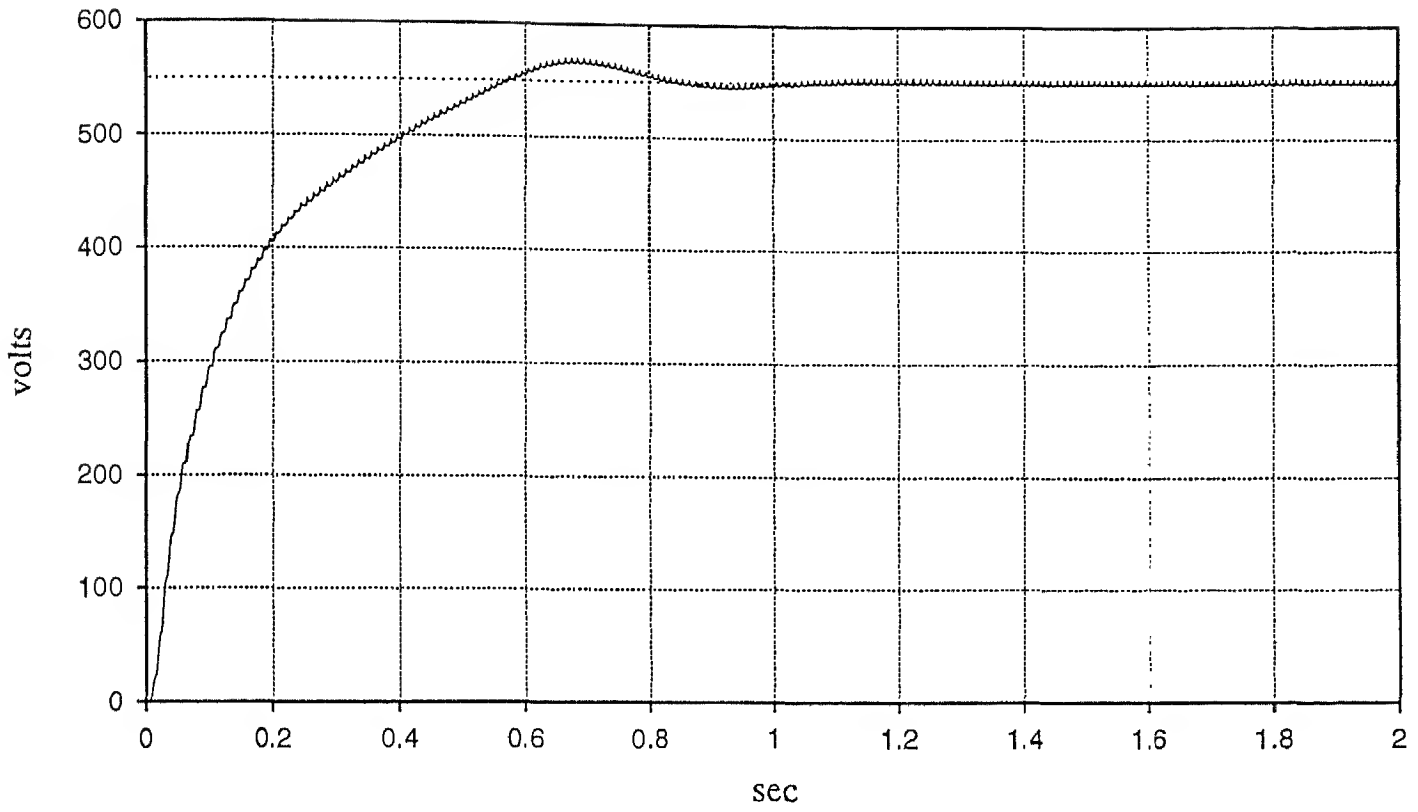

(b) Capacitor voltage (case-2)

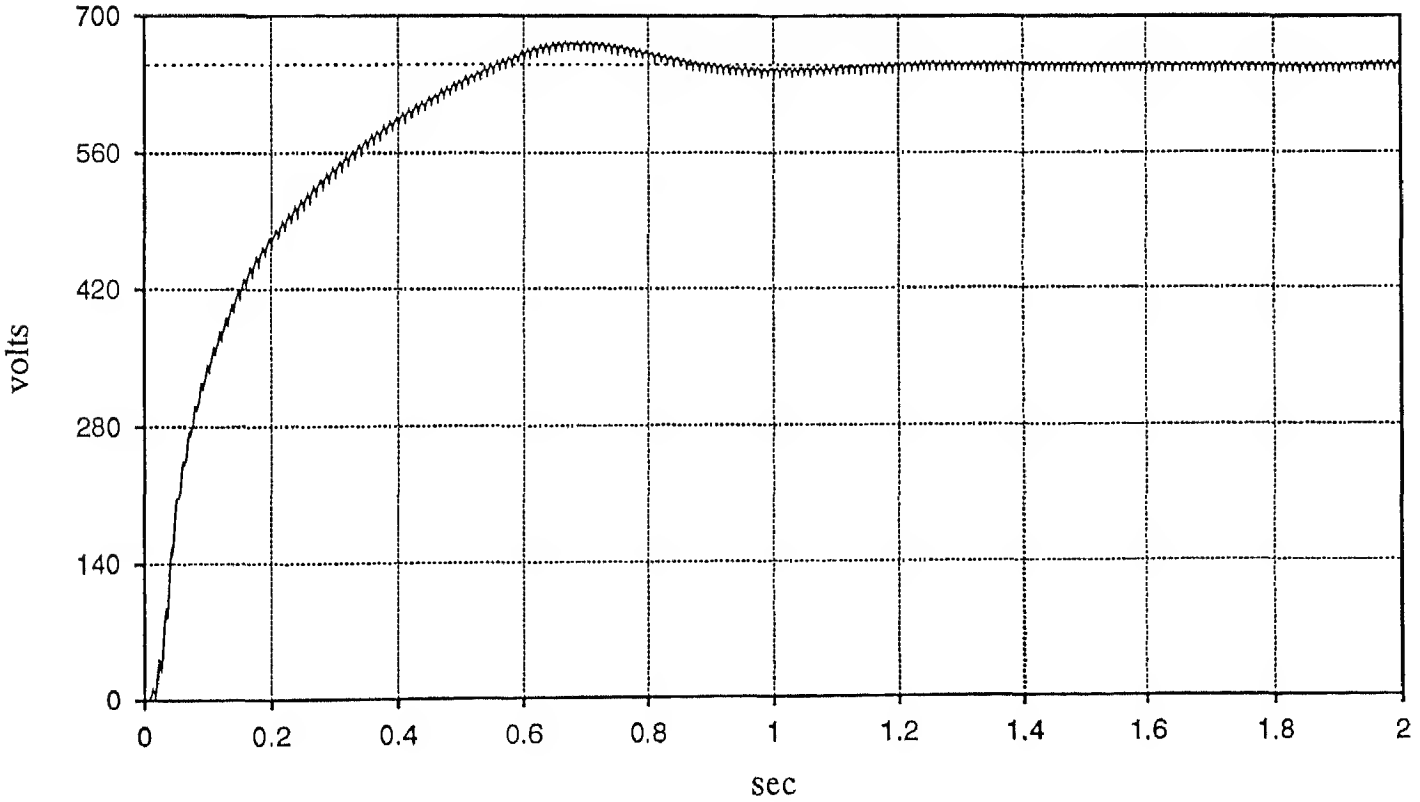

Fig. 2.8 Capacitor voltage variation during starting

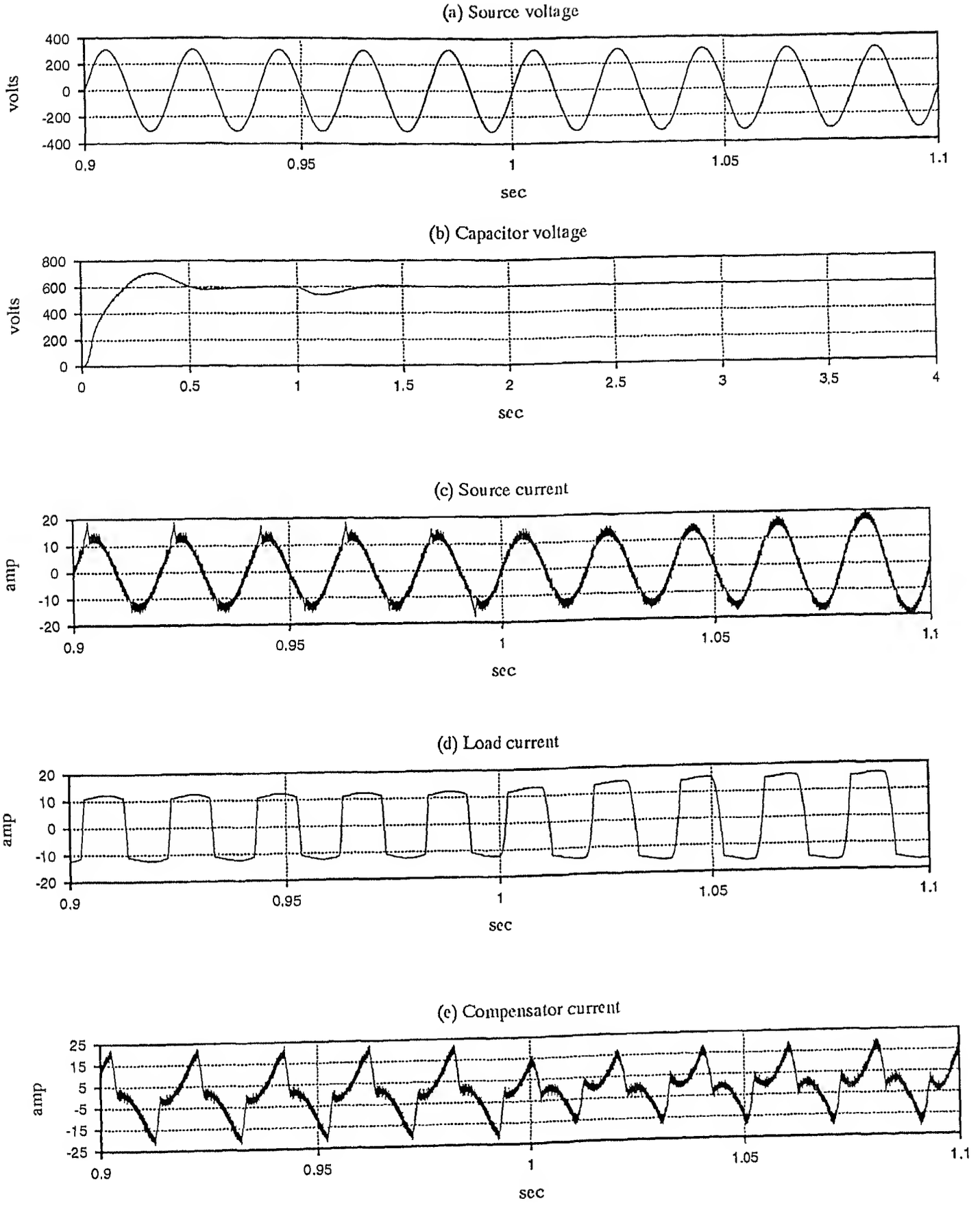

Fig.2.9 Simulated results during transient operating conditions

(For case-2, trigger algle is changed from 45 to 0 at 1.0 sec)

2.9 Conclusion

The following conclusions can be drawn from the analysis and simulation results presented in this chapter:

- The proposed active filter is able to supply the reactive power and compensate the harmonics drawn by the load, so that the current drawn by the source is sinusoidal and in phase with the source voltage. In $case-1$ the THD of the load current and the power factor were 69.3% and 0.7512 respectively. Whereas the THD and power factor of source current are 12.6% and 0.9922 respectively. For $case-2$ the above values are 33.2% and 0.7373, 7.2% and 0.9974.

- The current can be shaped only when the capacitor voltage is above a particular value.

- The lower order harmonics are eliminated and the frequencies of higher order harmonics present in the source current depends on the switching frequency of the power converter.

- The proposed active power filter operates with almost fixed switching frequency and is able to compensate current harmonics and the reactive power required by the load without computing the associated components of the load current.

Chapter 3

Three Phase Active Power Filter

3.1 Introduction

In the previous chapter, a single phase active power filter is discussed for harmonic elimination and power factor improvement. However the generation, transmission, distribution and utilization of large blocks of electric power are accomplished by means of three phase circuits. Recentaly various 3-phase active power filter configurations with their respective control strategies have been reported in the literature [13, 29, 40, 43]. Akagi et al [13] described an active power filter using multiple voltage source inverters and a time-delay PWM switching strategy. The control law is based on instantaneous reactive power theory [1]. Enjeti et al [29] have proposed an active power filter to cancel neutral current harmonics. The proposed approach employs a star/delta transformer along with a two-switch PWM-controlled active filter. Saetieo et al [43] have used sliding mode controller for active power filter implemetation. Moran et al [40] have used a tuned filter and PI controller for reference current generation and for current control strategy dc capacitor voltage controller and error triangulation technique.

In this chapter detailed analysis and simulation studies on three-phase active power filter is presented. The salient features of this active power filter are:

(i) The controller does not calculate the real, reactive or any harmonic or fundamental component of load current. Thus simplifying the control circuitry.

(ii) The current control is done using adaptive hysteresis band control technique [14], where in the switching frequency of the devices remain almost constant. This is achieved by varying the hysteresis band over the cycle.

(iii) The control is done in time domain which results in fast response.

(iv) Source current is forced to follow the reference current. whose magnitude depends only on the real power absorbed by the load and filter.

(v) The reference current is derived from the capacitor voltage control loop.

Typical simulation results are shown in this chapter to demonstrate the performance of the proposed active power filter.

3.2 Converter Model

The power circuit of the three-phase active power filter is shown in fig3.1. This consist of a three-phase inverter, a dc capacitor, and an inductor in each phase which links the inverter with the ac network. There are two control loops namely inner current control loop and outer capacitor voltage control loop.

The mid point of the DC side capacitor is connected to the ac neutral. Unequal distortion compensation can now be applied to each phase for unbalanced loads. Also the three line currents in individual phases can be controlled independently because there is no interaction between phase voltages of inverter leg.

From fig3.1, applying KVL for phases a,b,c of converter branch,

$$v_a = L\frac{di_{La}}{dt} + Ri_{La} + s_1\frac{v_d}{2} \tag{3.1}$$

$$v_b = L\frac{di_{Lb}}{dt} + Ri_{Lb} + s_2\frac{v_d}{2} \tag{3.2}$$

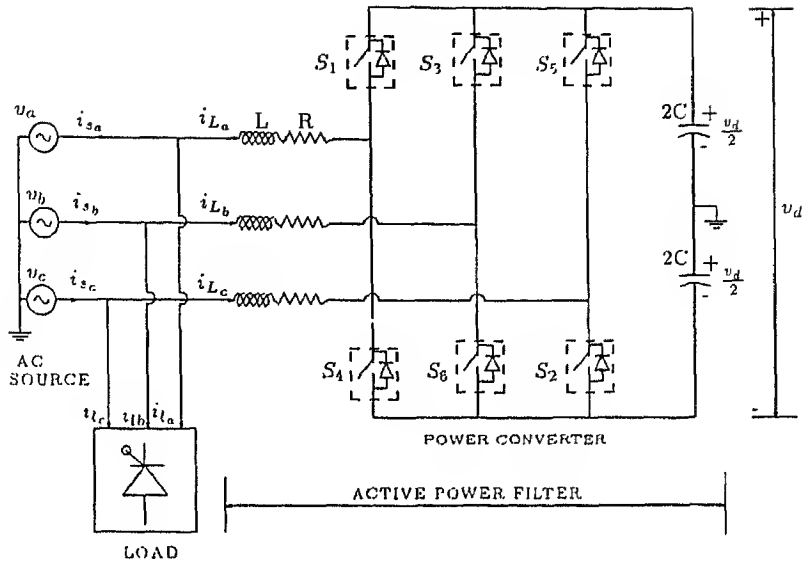

Figure 3.1: Power circuit of three-phase active power filter

$$v_c = L\frac{di_{Lc}}{dt} + Ri_{Lc} + s_3\frac{v_d}{2} \tag{3.3}$$

and on dc side:

$$2C\frac{dv_d}{dt} = s_1 i_{La} + s_2 i_{Lb} + s_3 i_{Lc} \tag{3.4}$$

The state-space representation of above equations can be written as:

$$\frac{d}{dt}\begin{bmatrix} i_{La} \\ i_{Lb} \\ i_{Lc} \\ v_d \end{bmatrix} = \begin{bmatrix} \frac{-R}{L} & 0 & 0 & \frac{-s_1}{2L} \\ 0 & \frac{-R}{L} & 0 & \frac{-s_2}{2L} \\ 0 & 0 & \frac{-R}{L} & \frac{-s_3}{2L} \\ \frac{s_1}{2C} & \frac{s_2}{2C} & \frac{s_3}{2C} & 0 \end{bmatrix} \begin{bmatrix} i_{La} \\ i_{Lb} \\ i_{Lc} \\ v_d \end{bmatrix} + \begin{bmatrix} \frac{v_a}{L} \\ \frac{v_b}{L} \\ \frac{v_c}{L} \\ 0 \end{bmatrix} \tag{3.5}$$

Where v_a, v_b, v_c are ac source voltages, which are given by

$$v_a = V_m sin(\omega t) \tag{3.6}$$

$$v_b = V_m sin(\omega t - \frac{2\pi}{3}) \tag{3.7}$$

$$v_c = V_m sin(\omega t + \frac{2\pi}{3}) \tag{3.8}$$

and i_{La}, i_{Lb}, i_{Lc} are 3-phase filter inductor currents, v_d is the capacitor voltage, s_1, s_2, s_3 are the switching functions, which are defined as:

$$s_1 = \begin{cases} 1 & if \quad S_1 \quad ON \\ -1 & if \quad S_2 \quad ON \end{cases} \tag{3.9}$$

$$s_2 = \begin{cases} 1 & if \quad S_3 \quad ON \\ -1 & if \quad S_6 \quad ON \end{cases} \tag{3.10}$$

$$s_3 = \begin{cases} 1 & if \quad S_5 \quad ON \\ -1 & if \quad S_2 \quad ON \end{cases} \tag{3.11}$$

In general, in any leg of the converter if upper switch is ON then $s_i = 1$, and if lower switch is ON then $s_i = -1$ (i=1,2,3). s_1, s_2, s_3 are independent control functions for phases a, b and c respectively. To increase the current in any phase the switch in the lower leg is turned ON and to decrease the current the switch in the upper leg is turned ON .

From equations (3.1), (3.2) and (3.3) , the inductor current can be controlled only if $(\frac{v_d}{2}) > (V_m)$. From equation (3.4), the capacitor voltage(v_d) will contain ripples. but its average value will be constant if the active power supplied by the source is the sum of active power drawn by the load and the inverter losses. The switching frequency of devices and the reactive power supplied by the inverter depends on the average value of the capacitor voltage.

3.3 Adaptive Hysteresis Band Current Control

From fig.(3.1), source current(i_s) is the sum of load current(i_l) and the inductor current(i_L). i.e.

$$i_s = i_l + i_L \tag{3.12}$$

or,

$$\frac{di_s}{dt} = \frac{di_l}{dt} + \frac{di_L}{dt} \tag{3.13}$$

$$= \frac{di_l}{dt} + \frac{1}{L}\left(v_s - Ri_L - s\frac{v_d}{2}\right) \tag{3.14}$$

$$= \frac{1}{L}\left(v_s - Ri_L + L\frac{di_l}{dt} - s\frac{v_d}{2}\right) \tag{3.15}$$

To increase the current(i_s) $s = -1$. Therefore

$$\frac{di_s^+}{dt} = \frac{1}{L}\left(v_s - Ri_L + L\frac{di_l}{dt} + \frac{v_d}{2}\right) \tag{3.16}$$

and to decrease the current(i_s) $s = 1$. Therefore

$$\frac{di_s^-}{dt} = \frac{1}{L}\left(v_s - Ri_L + L\frac{di_l}{dt} - \frac{v_d}{2}\right) \tag{3.17}$$

The general expression for hysteresis band(HB) can be written as:

$$HB = \left(\frac{0.25\left(\frac{v_d}{2}\right)}{f_s L}\right)\left(1 - \left(\frac{v_s - Ri_L + L\frac{di_l}{dt} - L\frac{di_s^*}{dt}}{\frac{v_d}{2}}\right)^2\right) \tag{3.18}$$

and for individual phases a, b, c the hysteresis band can be written as:

$$HB_a = \left(\frac{0.25\left(\frac{v_d}{2}\right)}{f_s L}\right)\left(1 - \left(\frac{v_a - Ri_{La} + L\frac{di_{l_a}}{dt} - L\frac{di_{s_a}^*}{dt}}{\frac{v_d}{2}}\right)^2\right) \tag{3.19}$$

$$HB_b = \left(\frac{0.25\left(\frac{v_d}{2}\right)}{f_s L}\right)\left(1 - \left(\frac{v_b - Ri_{Lb} + L\frac{di_{l_b}}{dt} - L\frac{di_{s_b}^*}{dt}}{\frac{v_d}{2}}\right)^2\right) \tag{3.20}$$

and

$$HB_c = \left(\frac{0.25\left(\frac{v_d}{2}\right)}{f_s L}\right)\left(1 - \left(\frac{v_c - Ri_{Lc} + L\frac{di_{l_c}}{dt} - L\frac{di_{s_c}^*}{dt}}{\frac{v_d}{2}}\right)^2\right) \tag{3.21}$$

The three-phase current control strategy is given in Table:3.1. If for a given phase, the current error($\Delta i = i^* - i_{actual}$) is greater than the hysteresis band, the lower switch of the inverter leg corresponding to that phase is turned *ON*, and if the current error is less than the negative of the hysteresis band then the upper switch is turned *ON*. If the error is with in the hysteresis band previous switching state is retained.

Table 3.1: Adaptive Hysteresis Band Current Control Rule

If	*Then Switch ON*
$\Delta i_a > HB_a$	S_4
$\Delta i_a < HB_a$	S_1
$-HB_a \leq \Delta i_a \leq HB_a$	No change
$\Delta i_b > HB_b$	S_6
$\Delta i_b < HB_b$	S_3
$-HB_b \leq \Delta i_b \leq HB_b$	No change
$\Delta i_c > HB_c$	S_2
$\Delta i_c < HB_c$	S_5
$-HB_c \leq \Delta i_c \leq HB_c$	No change

3.4 Reference Current Generation and Capacitor Voltage Control Loop

The reference current generation philosophy is the heart of the active power filter control circuitry. Similar to the single phase case, capacitor voltage(v_d) is filtered to get its average dc value V_d and then subtracted from the reference voltage(V_c^*). The error voltage($\Delta V_d = V_c^* - V_d$) thus obtained is fed to a proportional-integral(PI) controller. The reference source current for a particular phase is obtained by multiplying the output(k) of the PI controller by sin(ωt). The three reference waveforms are displaced by $2\pi/3$ radians from each other. The expression for three reference currents can be written as:

$$i_{sa}^* = k sin(\omega t) \tag{3.22}$$

$$i_{sb}^* = k sin(\omega t - \frac{2\pi}{3}) \tag{3.23}$$

and

$$i_{sc}^* = k sin(\omega t + \frac{2\pi}{3}) \tag{3.24}$$

$$or$$

$$i^*_{sc} = -i^*_{sa} - i^*_{sb} \tag{3.25}$$

Using the adaptive current controller, the source currents are forced to track the above reference currents. This ensures that irrespective of load current waveform, the source current is sinusoidal and in phase with the supply voltages.

3.5 Simulation Results

To prove the validity of the proposed active filtering scheme, the simulation was done on PSCAD/$EMTDC^{TM}$. The three phase active power filter was tested for three different types of non-linear loads:

(i) $3-phase$ diode rectifier with dc side filter capacitor and resistive load,

(ii) $3-phase$ controlled rectifier, and

(iii) unbalanced load: $R-L$ load in $phase-a$ and a diode rectifier between $phases-b$ and c.

In each case the ac source voltage is maintained at $220V$ per phase.

3.5.1 Case-1

Fig.3.2 shows the complete block diagram in which the active filter is compensating the 3-phase diode rectifier. The block diagram is simulated and the results are shown in fig.3.3. The current drawn by the load is shown in fig.3.3(d) and its harmonic spectrum is in fig.3.3(f). The source current and its harmonic spectrum are shown in fig.3.3(c) & (e). The THD of the load current and the source current are found to be 26.6% and 7.3% respectively. The load power factor and supply power factor are found to be 0.65329 and 0.9974 respectively. The parameters of the active filter were: $f_s = 6kHz, 2C = 2000\mu F, L = 20mH, K_p = 0.1$ and $K_i = 1.0, V_c^* = 900V$.

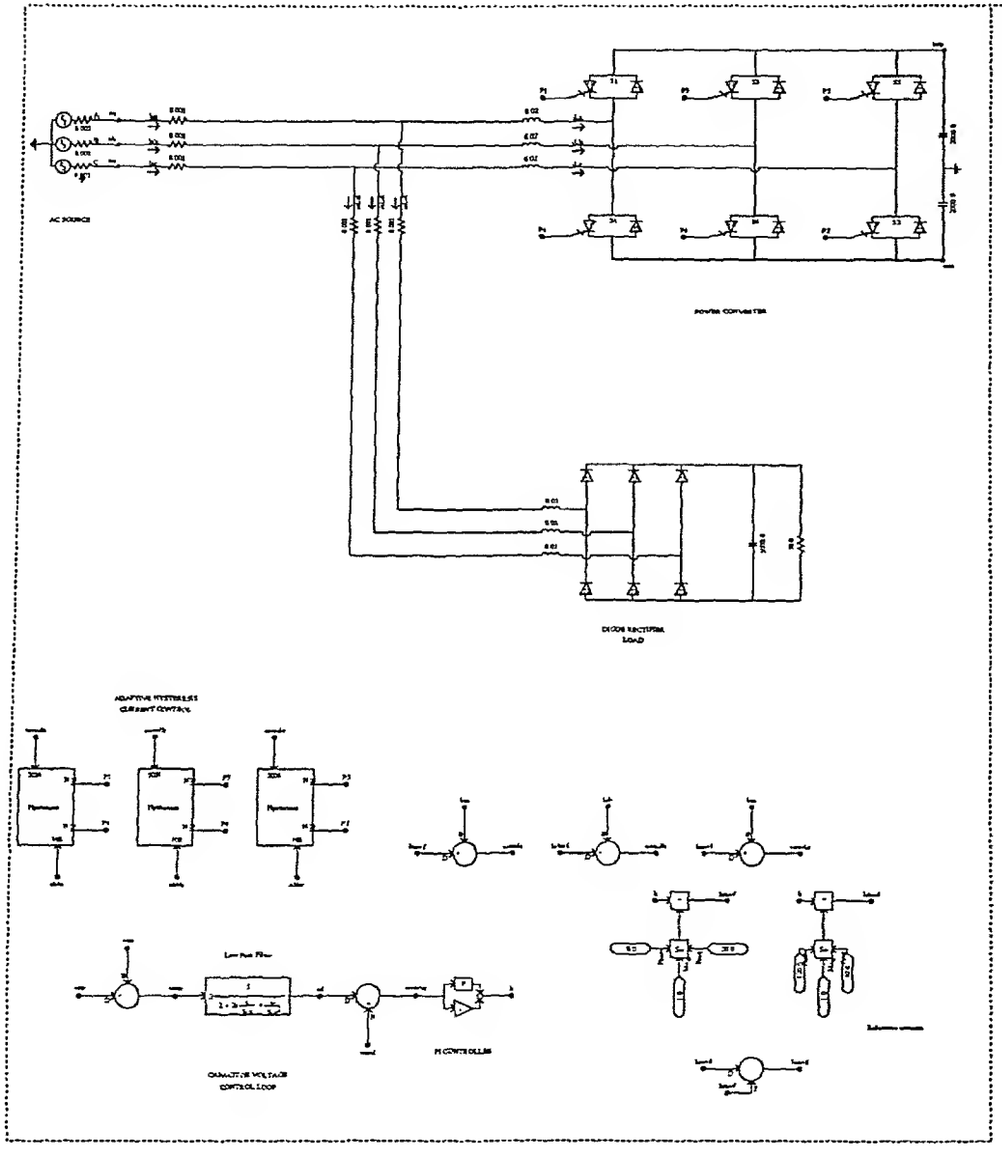

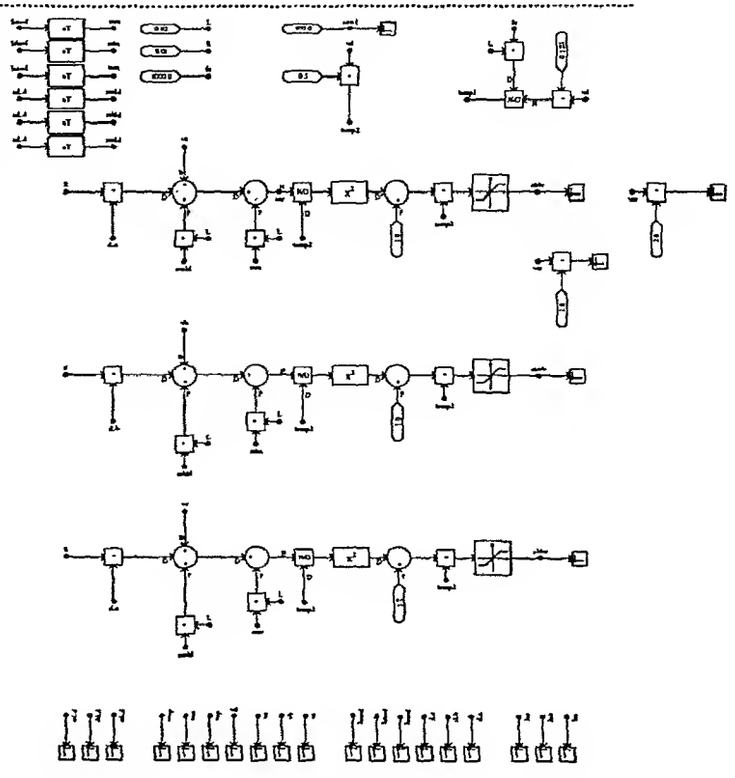

Figure 3.2: Block diagram for case-1

IIT Kanpur, INDIA *1-Phase*	Created: November 14, 1995 (shym) Last Modified: January 19, 1996 (shym) Printed On: January 19, 1996 (shym)	*SS 1*

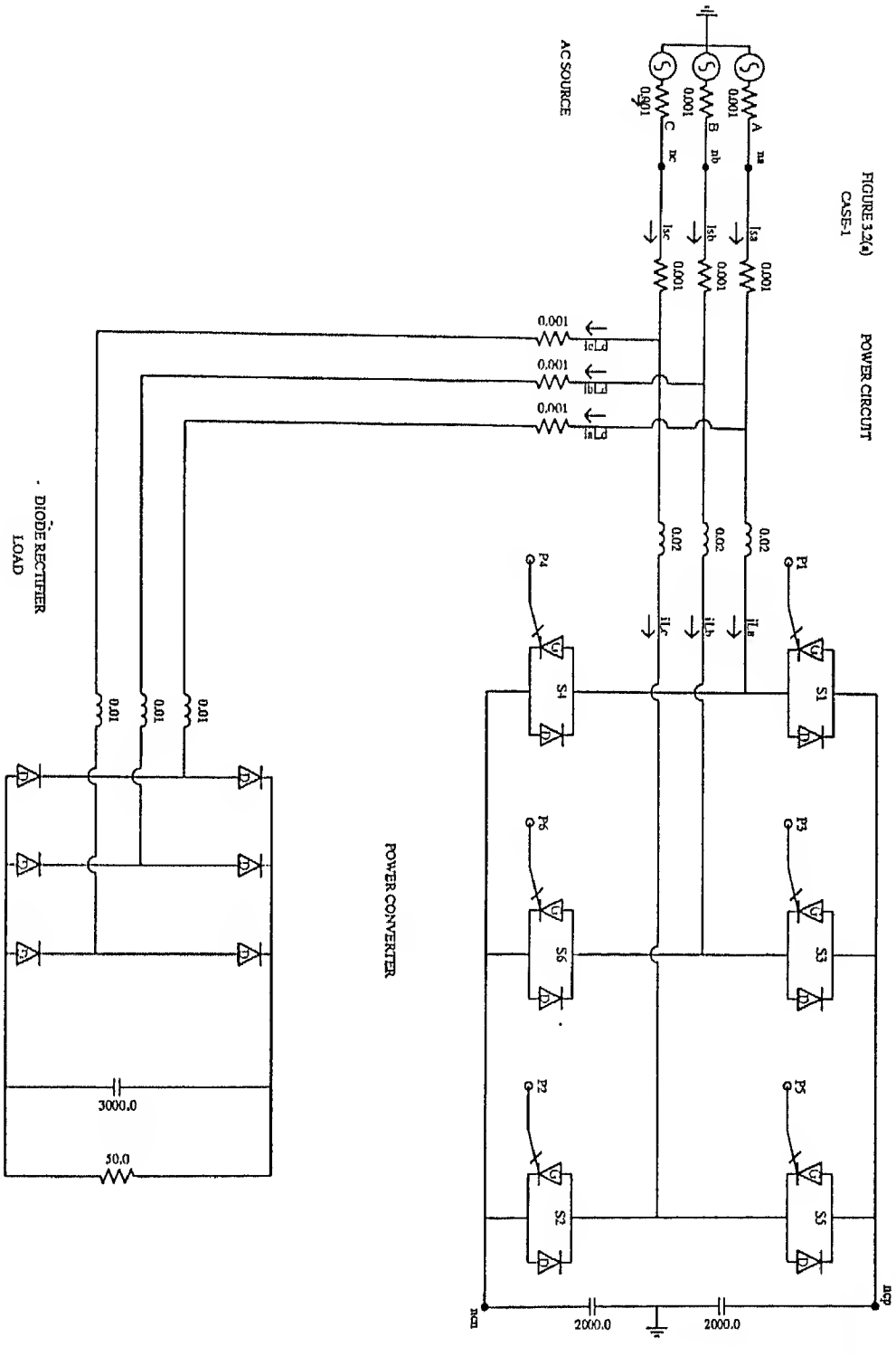

IIT Kanpur, INDIA *1-Phase*	Created: Last Modified: Printed On:	November 14, 1995 (shym) January 31, 1996 (shym) January 31, 1996 (shym)
SS 1		
		Page 1 of 4

FIGURE 3.2(b)
CASE-1

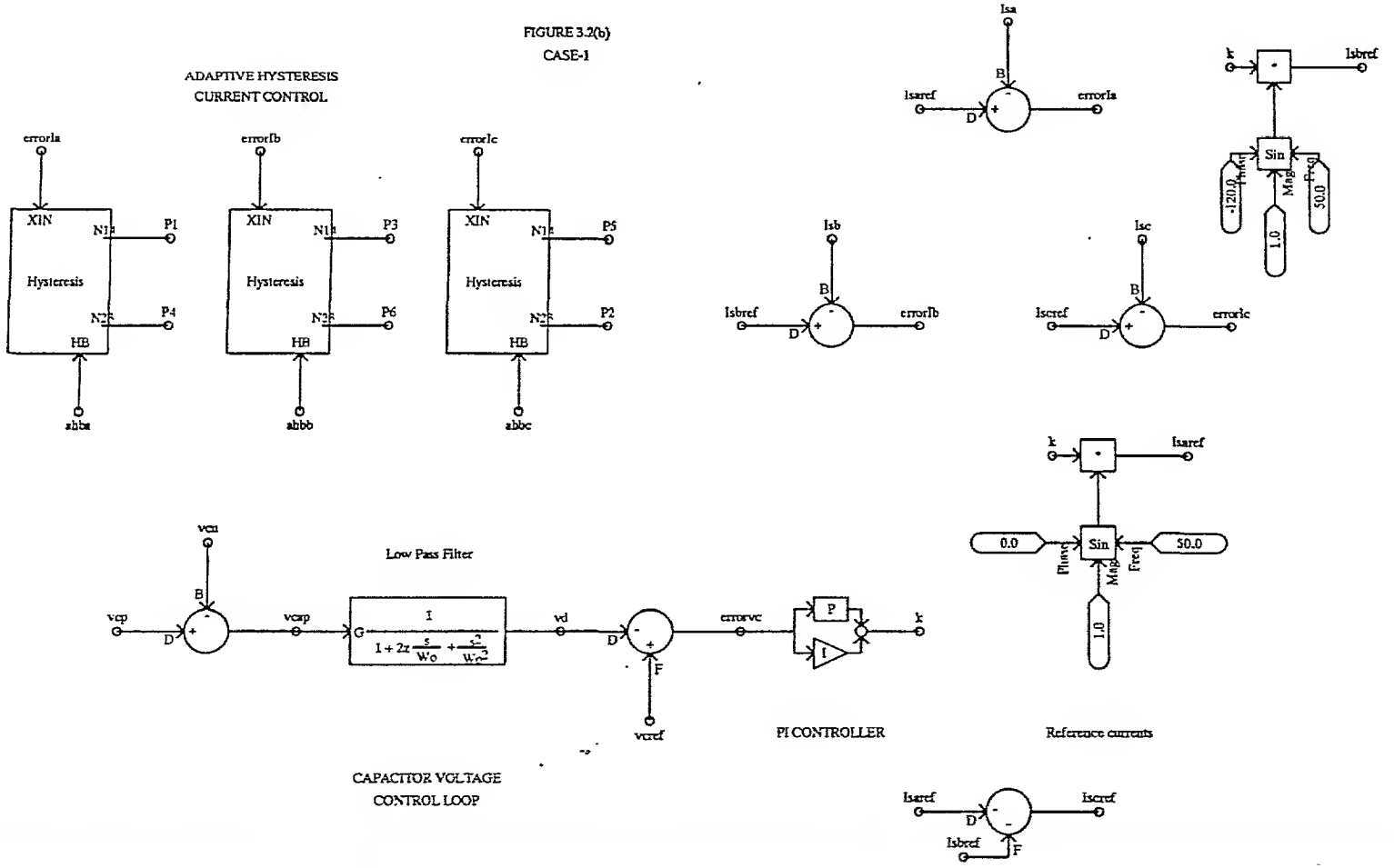

35-C

FIGURE 3.2(c)
CASE-1

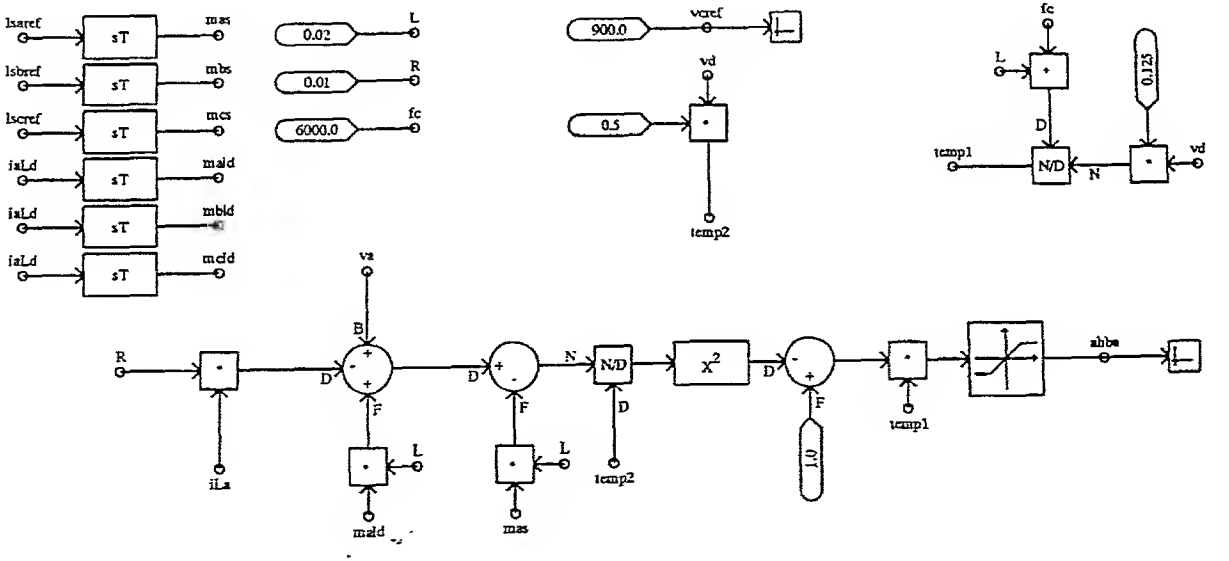

IIT Kanpur, INDIA *1-Phase*	Created: Last Modified: Printed On:	November 14, 1995 (shym) January 31, 1996 (shym) January 31, 1996 (shym)	*SS 1* Page 2 of 4

FIGURE 3.2(d)
CASE-I

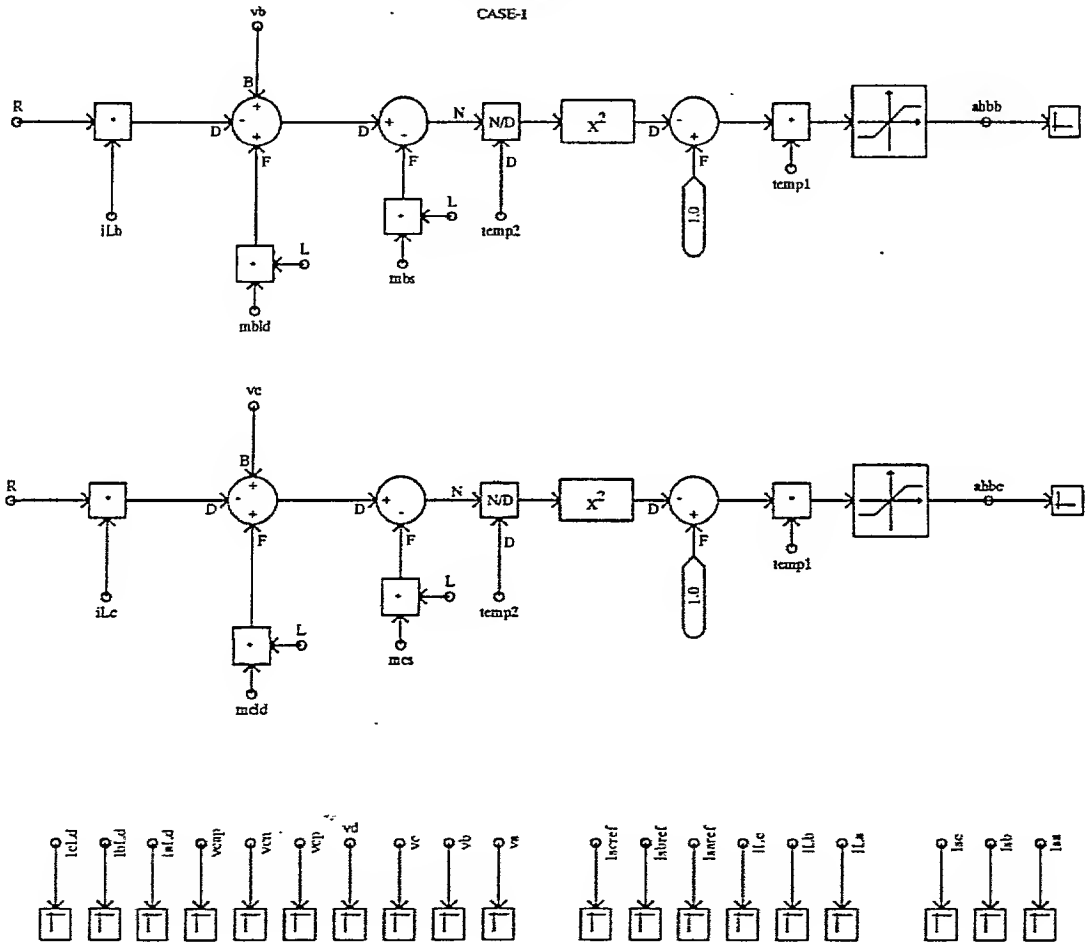

IIT Kanpur, INDIA *1-Phase*	Created: Last Modified: Printed On:	November 14, 1995 (shym) January 31, 1996 (shym) January 31, 1996 (shym)	*SS 1*

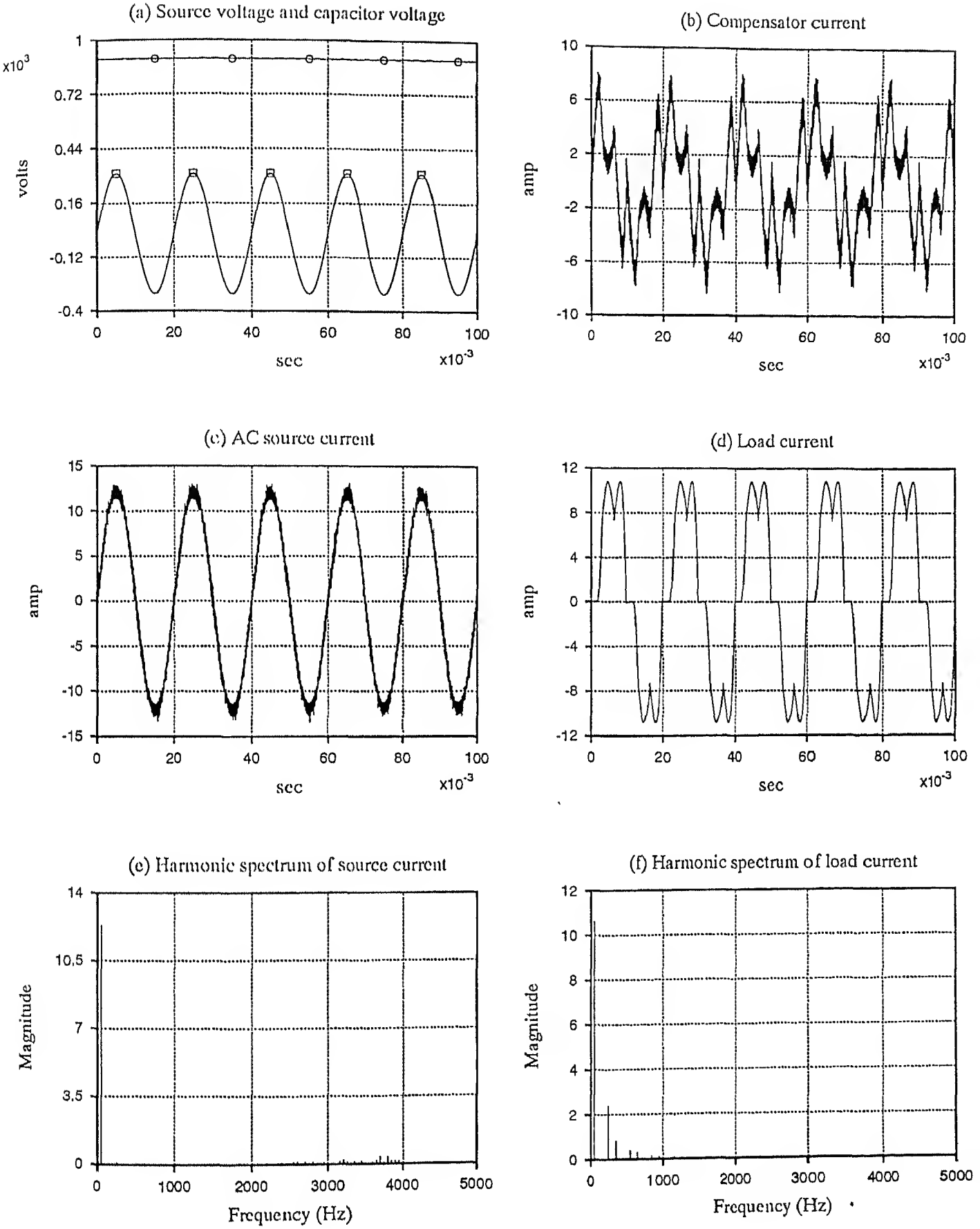

Fig. 3.3 Simulated results for case-1 (phase-a)

3.5.2 Case-2

Active power filter compensating the harmonics and reactive power drawn by a three phase thyristor bridge rectifier from the source is studied and the simulated results are shown in fig.3.5. The load current waveform, its harmonic spectrum are shown in fig.3.5(d) & (f) respectively and current drawn by source and its harmonic spectrum in fig3.5(c) & (e) respectively. The THD of load current and source current are are found to be 24.8% and 10.6% respectively and the power factor of source current and load current are 0.996 and 0.52 respectively. This reduction in harmonic content and reactive power drawn from the source is due to active power filter. The current waveform drawn by the filter is shown in fig.3.5(b). The parameters of the active filter are: $f_s = 6kHz, 2C = 2000\mu F, L = 20mH. K_p = 0.1, K_i = 1.0$ and $V_c^* = 1500V$.

3.5.3 Case-3

Performance of the active power filter is also evaluated for unbalanced loads. The block diagram of active filter compensating the harmonic and reactive power drawn by the unbalanced load is shown in fig.3.6. A diode bridge rectifier is connected to phases b & c and $R-L$ load is connected to phase$-a$. The respective load currents, source currents and the compensator currents in phases a , b, c are shown in fig.3.7(g), (h). (i) ; fig.3.7(d), (e), (f) and fig.3.7(j), (k), (l) respectively. The THD in load current in phase b & c is 34.2%, and power factor of the load connected to phase a, b & c are found to be 0.5132, 0.94104 & 0.55521 respectively. Whereas THD in the source current and its power are 10.4% and 0.9946 respectively. The parameters of the active power filter were: $f_s = 6kHz, 2C = 2000\mu F, L = 20mH, K_p = 0.1$, $K_i = 1.0$ and $V_c^* = 900V$.

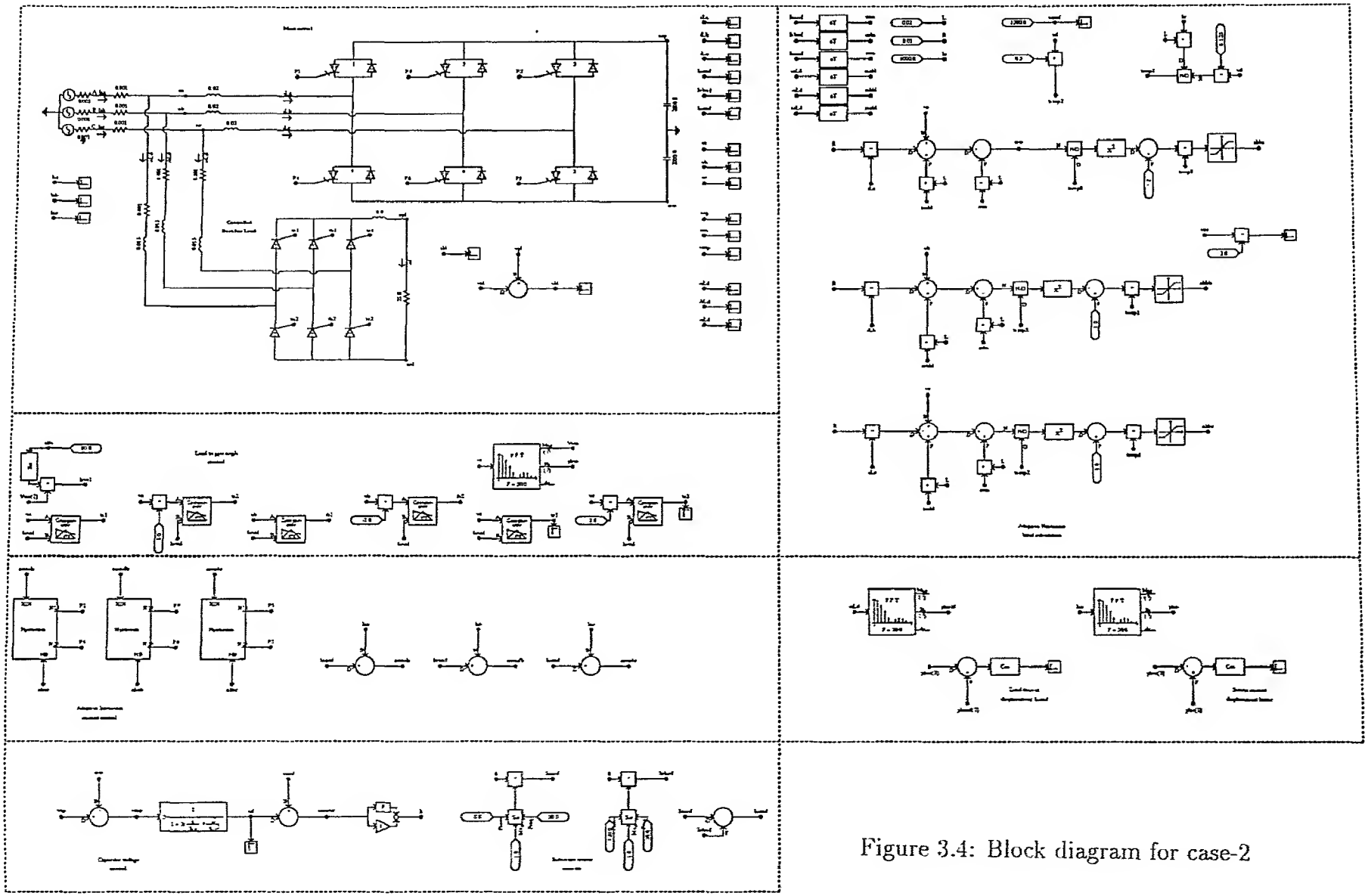

Figure 3.4: Block diagram for case-2

IIT Kanpur, INDIA *1-Phase*	Created: November 14, 1995 (shym) Last Modified: January 19, 1996 (shym) Printed On: January 19, 1996 (shym)	*SS 1*

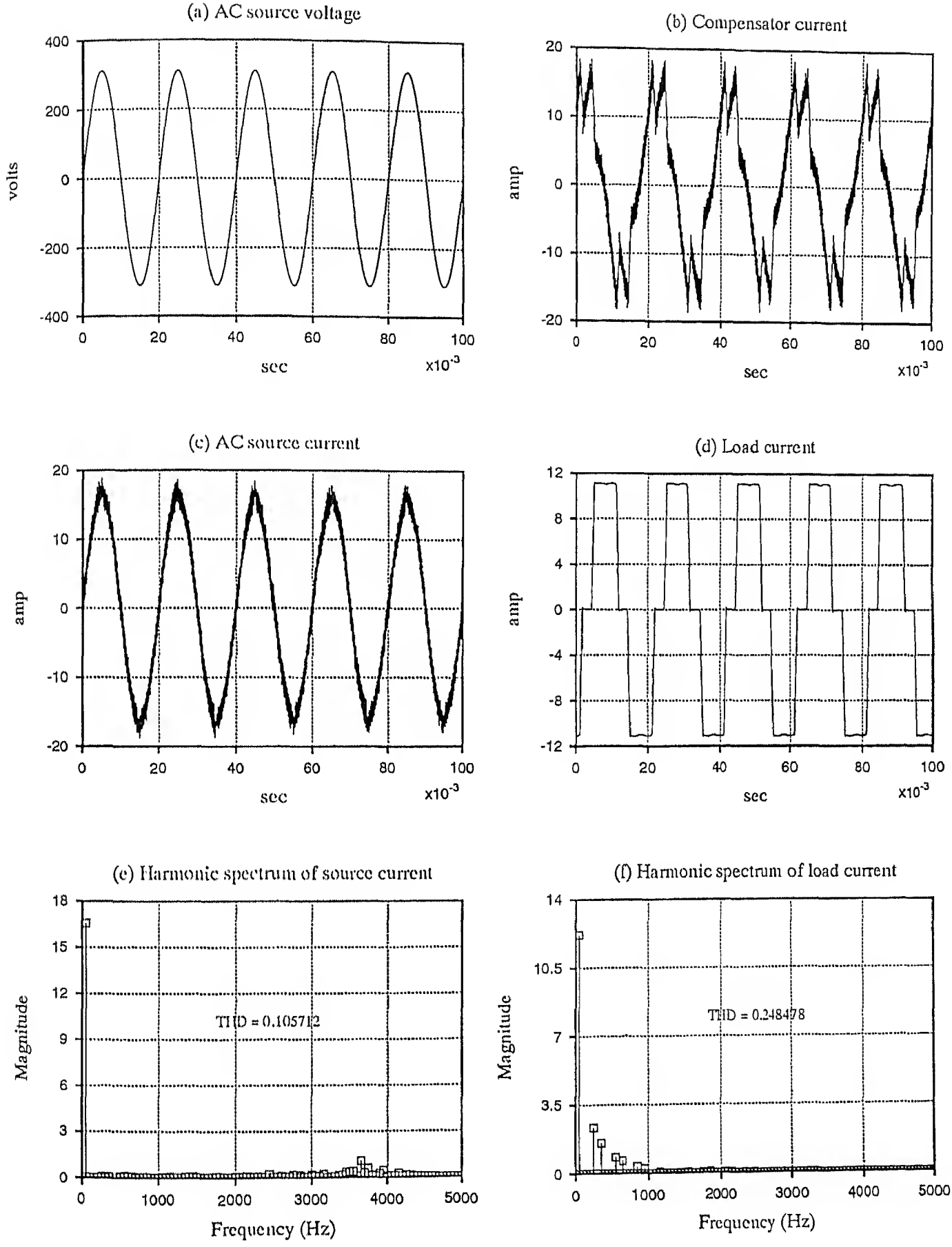

Fig.3.5 Simulation results for case-2 (phase-a)

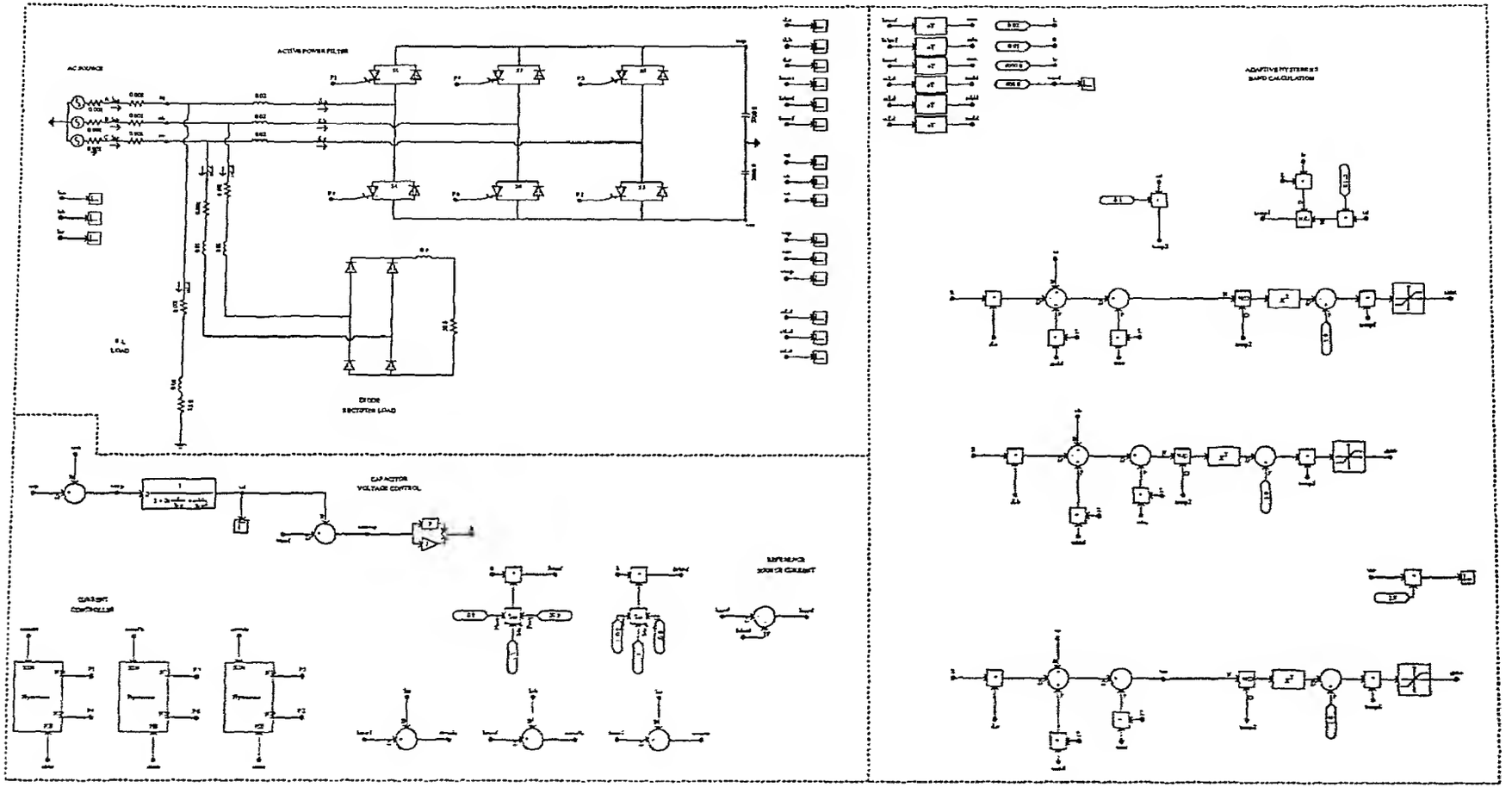

Figure 3.6: Block diagram for case-3 (Unbalanced load)

IIT Kanpur, INDIA *1-Phase*	Created: November 14, 1995 (shym) Last Modified: January 19, 1996 (shym) Printed On: January 19, 1996 (shym)	*SS 1*

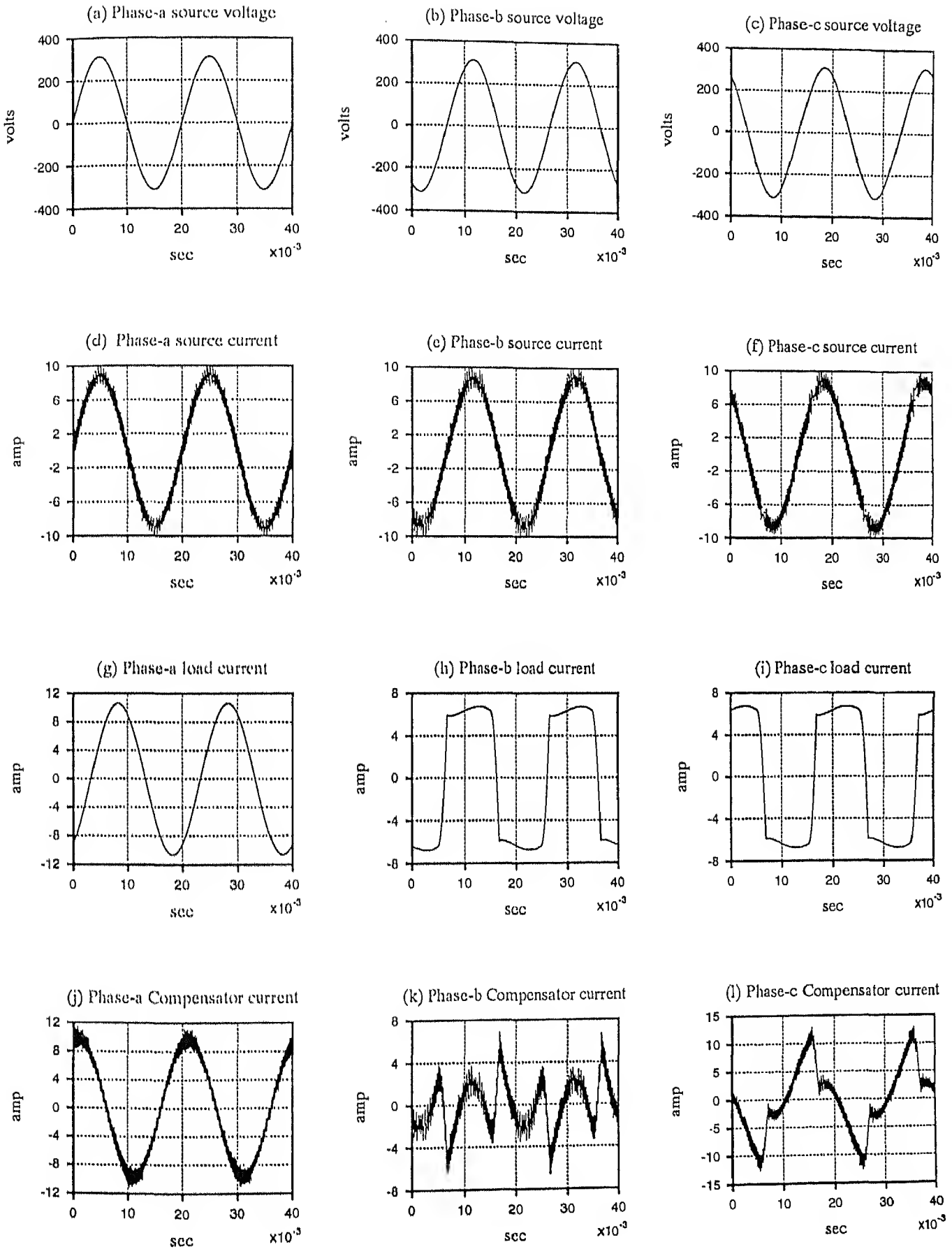

Fig.3.7 Simulated results for case-3 (Unbalanced load)

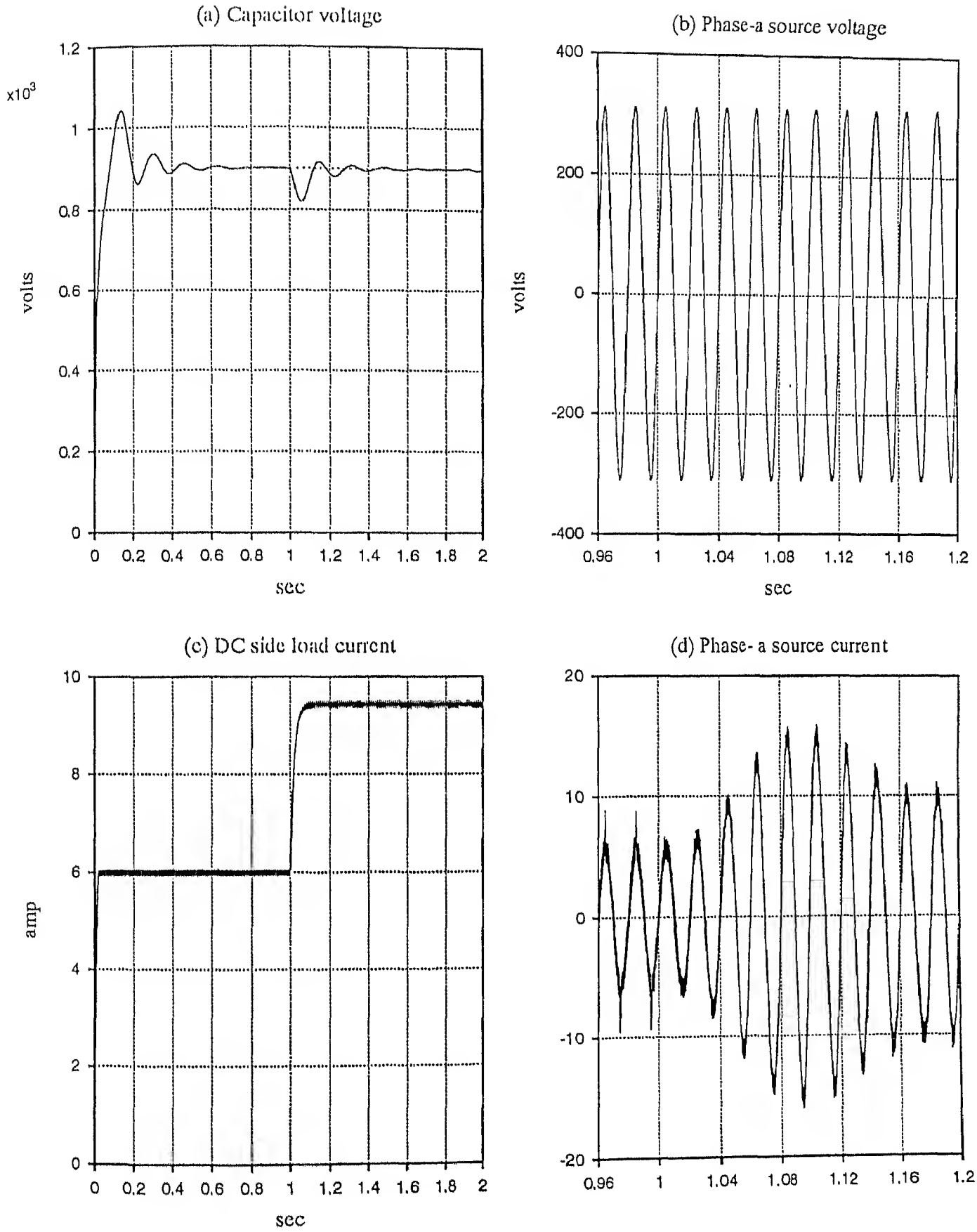

Fig. 3.8 Simulated results during transient operating conditions

(For case-2, trigger angle changed from 80 to 30 at 1.0 sec)

3.5.4 Performance of the Filter During Transient Condition

Fig.3.8 shows the simulated current and capacitor voltage waveforms during transient conditions. Initially the active power filter was compensating a bridge rectifier load whose trigger angle was maintained at 80 deg. At $t = 1$ sec the trigger angle is changed to 30 deg. which results in increase in the load current. Initially this increase in the load current is supplied by the capacitor. As a result the capacitor voltage falls. The PI controller generates higher reference current. This increase in reference source current will maintain the capacitor voltage to its reference value. It is also evident from the fig3.8(b) and fig3.8(d) that the source current is sinusoidal and in phase with the voltage during transient condition.

3.6 Conclusion

From the analysis and simulation carried out in this chapter the following conclusions are made:

- Due to the compensating action of the active filter, it is found that the source power factor is approximately equal to unity. Also there is a significant improvement in the THD in the source current.
- The displacement factor of the source current is found to be unity. It can be inferred that the total reactive power of the load is supplied by the compensator.
- The proposed active power filter is able to compensate for unbalanced nonlinear loads.
- The proposed active power filter is able to compensate for the reactive power and harmonics without analysing the load current.
- The capacitor voltage control loop is able to make the source current to be sinusoidal and in phase with voltage.
- The active power filter operates with almost constant switching frequency. This is achieved using an adaptive hysteresis band current controller.

Chapter 4

Conclusion

4.1 General

Effects of harmonic pollution and operation at low power factor on power system are well known. These problems are aggravated due to the increased use of loads fed by converter/inverter. Active power filters are increasingly being used to solve the above problems.

In this chapter the main results of the work carried out in this thesis and suggestions for further work in this area are discussed.

- Single phase and three-phase active power filters are studied for harmonic and reactive power compensation. They are able to reduce the current harmonic distortion and the reactive power demand of the load significantly. This results in improvement of source power factor.

- Adaptive hysteresis band current controller is used. This controller operates the inverter at constant switching frequency.

- The controller generates the reference source current without determining the reactive or active or any harmonic component of the load curent.

- Single phase active power filter is analysed and simulated for two types of non-linear loads. In each case the filter functions as harmonic and reactive power compensator satisfactorily. The same is true for three-phase active power filter.

4.2 Scope for future work

Further work can be attempted in the following areas:

- Operation of active power filter in combination with the passive filters.
- Experimental investigation of the active power filter without analysing the load current.
- Predictive current control strategy for current control.
- Detailed mathematical analysis of the filter with power and control circuits.
- Operation at optimum source power factor when the filter $KVar$ rating is less than the reactive power demand of the load without measuring the load current components.

Bibliography

[1] Hirofumi Akagi, Yoshihira Kanazawa and Akira Nabae, *"Instantaneous Reactive Power Compensators Comprising Switching Devices without Energy Storage Components"*, IEEE Trans. on Industry Applications, Vol. 20, No.3, May/June 1984, pp. 625-630.

[2] Atsuo Kawamura and Richard Hoft, *"Instantaneous Feedback Controlled PWM Inverter with Adaptive Hysteresis"*, IEEE Trans. on Industry Applications. Vol. 20, No. 4, July/August 1984, pp. 769-775.

[3] David M. Brod and Donald W. Novotny, *"Current Control of VSI-PWM Inverters"*, IEEE Trans. on Industry Applications. Vol. 21, No. 4, May/June 1985. pp. 562-570.

[4] Hirofumi Akagi, Akira Nabae and Satoshi Atoh, *"Control Strategy of active power filters using multiple voltage-source PWM converters"*, IEEE Trans. on Industry Applicatios, Vol. 22, No. 3, May/June 1986, pp. 460-465.

[5] Akira Nabae, Satoshi Ogasawara and Hirofumi Akagi, *" A Novel Control Scheme for Current-Controlled PWM Inverters"*, IEEE Trans. on Industry Applications, Vol. 22, No. 4, July/August 1986, pp. 697-701.

[6] Boon Teck Ooi, John C. Salmon, Juan W. Dixon and Ashok B. Kulkarni, *"A three-phase controlled-current PWM converter with leading power factor"* , IEEE Trans. on Industry Applications, Vol. 23, No. 1, Jan/Feb. 1987, pp. 78-84.

[7] Gyu-Ha and Min-Ho Park, *"A new injection method for ac harmonic elimination by active power filter"*, IEEE Trans. on Industrial Electronics, Vol. 35, No. 1, February 1988, pp. 141-147.

[8] Juan W. Dixon and Boon-Teck Ooi, *"Indirect current control of a unity power factor sinusoidal current boost type three-phase rectifier"*, IEEE Trans. on Industrial Electronics, Vol. 35, No. 4, November 1988, pp. 508-515.

[9] Omar Stihi and Boon-Teck Ooi, *"A single-phase controlled-current PWM rectifier"*, IEEE Trans. on Power Electronics, Vol. 3, No. 4, October 1988, pp. 453-459.

[10] J.T.Boys and A.W.Green, *"Current-forced single-phase reversible rectifier"*, IEE Proceedings, Vol. 136, Pt.B, No. 5, September 1989, pp. 205-211.

[11] Hoang Le-Huy and Louis A. Dessaint. *"An Adaptive Current Control Scheme for PWM Synchronous Motor Drives: Analysis and Simulation"*, IEEE Trans. on Power Electronics, Vol. 4, No. 4, October 1989, pp. 486-495.

[12] Gyu-Ha and Min-Ho Park, *"Analysis and control of active power filter with optimised injection"*, IEEE Trans. on Power Electronics, Vol. 4, No. 4, October 1989, pp. 427-433.

[13] Hirofumi Akagi, Yukifumi Tsukamoto and Akira Nabae, *"Analysis and Design of an Active Power Filter Using Quad-Series Voltage Source PWM Converters"*, IEEE Trans. on Industry Applications. Vol. 26, No. 1, January/February 1990. pp. 93-98.

[14] Bimal K. Bose, *"An Adaptive Hysteresis-Band Current Control Technique of a Voltage-Fed PWM Inverter for Machine Drive System"*, IEEE Trans. on Industrial Electronics, Vol. 37, No. 5, October 1990, pp. 402-408.

[15] W.M.Grady, M.J.Samotyj and A.H.Noyola, *"Survey of Active Power Line Conditioning Methodologies,* IEEE Trans. on Power Delivery", Vol. 5. No. 3. July 1990, pp. 1536-1542.

[16] Luigi Malesani and Paolo Tenti, *"A Novel Hysteresis Control Method for Current-Controlled Voltage-Source PWM Inverters with Constant Modulation Frequency"*, IEEE Trans. on Industry Applications, Vol. 26, No. 1, January/ February 1990, pp. 88-92.

[17] Rusong Wu, Shashi B. Dewan and Gordon R. Slemon, *"A PWM AC-DC Converter with Fixed Switching Frequency"*. IEEE Trans. on Industry Applications, Vol. 26, No. 5, September/October 1990, pp. 880-885.

[18] Mehrdad Kazerani, Phoivos D. Ziogas and Geza Joos, *"A Novel Active Current Waveshaping for Solid-State Input Power Factor Conditioners"*, IEEE Trans. on Industrial Electronics, Vol. 38, No. 1, February 1991, pp. 72-78.

[19] Marian P. Kazmierkowski, Maciej A. Dzieniakowski and Waldemar Sulkowski, *"Novel Space Vector Based Current Controllers for PWM-Inverters"*, IEEE Trans. on Power Electronics, Vol. 6, No. 1, January 1991, pp. 158-166.

[20] Luigi Malesani, Leopoldo Rossetto and Paolo Tenti, *"Active Power Filter with Hybrid Energy Storage"*, IEEE Trans. on Power Electronics, Vol. 6, No. 3, July 1991, pp. 392-397.

[21] Masayuki Morimoto, Kiyotaka Sumito, Shinji Sato, Katsumi Oshitani, Muneaki Ishida, Shigeru Okuma, *"High efficiency, unity power factor VVVF drive system of an induction motor"*, IEEE Trans. on Power Electronics, Vol. 6, No. 3. July 1991, pp. 498-503.

[22] A. R. Prasad, Phoivos D. Ziogas and Stefanos Manias, *"An Active Power Factor Correction Technique for Three-phase Diode Rectifiers"*, IEEE Trans. on Power Electronics, Vol. 6, No.1, January 1991, pp. 83-92.

[23] Eugenio Wernekinck, Atsuo Kawamura and Richard Hoft, *"A High Frequency AC/DC Converter with Unity Power Factor and Minimun Harmonic Distortion"*, IEEE Trans. on Power Electronics, Vol. 6. No. 3, July 1991. pp. 364-370.

[24] Bimal K. Bose, *"Recent Advances in Power Electronics"*, IEEE Trans. on Power Electronics, Vol. 7, No. 1, January 1992, pp. 2-16.

[25] Richard M. Duke and Simon D. Round, *"The steady-state performance of a controlled current active filter"*, IEEE Trans. on Power Electronics, Vol. 8. No. 3. April 1993, pp 140-146.

[26] Geza Joos and Phoivos D. Ziogas, *"On Maximizing Gain and Minimizing Switching Frequency of Delta Modulated Inverters"*, IEEE Trans. on Industrial Electronics, Vol. 40, No. 4, August 1993, pp. 436-444.

[27] Luis Moran, Phoivos D. Ziogas and Geza Joos, *"A solid-state high-performance reactive-power compensator"*, IEEE Trans. on Industry Applications. Vol. 29, No. 5, Sep/Oct 1993, pp. 969-978.

[28] Hirofumi Akagi, *"Trends in Active Power Line Conditioners,* IEEE Trans. on Power Electronics, Vol.9, No.3, May 1994, pp. 263-268.

[29] Prasad N. Enjeti, Wajiha Shireen, Paul Packebush and Ira J. Pitel, *"Analysis and Design of a New Active Power Filter to Cancel Neutral Current Harmonics in a Three-Phase Four-Wire Electric Distribution Systems"*, IEEE Trans. on Industry Applications, Vol. 30, No. 6, November/December 1994, pp. 1565-1572.

[30] Hoang Le-Huy, Karim Slimani and Philippe Viarouge, *"Analysis and Implementation of a Real-Time Predictive Current Controller for Permanent- Magnet Synchronous Servo Drives"*, IEEE Trans. on Industrial Electronics, Vol. 41, No. 1, February 1994, pp. 110-117.

[31] Sikyung Kim, Prasad N. Enjeti, Paul Packebush and Ira J. Pitel, *"A New Approach to Improve Power Factor and Reduce Harmonic in a Three-Phase Diode Rectifier type Utility Interface"*, IEEE Trans. on Industry Applications, Vol. 30, No. 6, November/December 1994, pp. 1557-1564.

[32] Janko Nastran, Rafael Cajhen, Matija Seliger and Peter Jereb, *"Active power filter for nonlinear ac loads"*, IEEE Trans. on Power Electronics, Vol. 9. No. 1, January 1994, pp. 92-96.

[33] Ching-Tsai Pan, Ting-Yu Chag, *"An improved hysteresis current controller for reducing switching frequency"*, IEEE Trans. on Power Electronics. Vol. 9. No. 1. January 1994. pp. 97-104.

[34] Mukul Rastogi, Rajendra Naik and Ned Mohan, *"A comparative Evaluation of harmonic reduction techniques in three-phase utility interface of power electronic loads"*, IEEE Trans. on Industry Applications, Vol. 30, No. 5, September/October 1994. pp. 1149-1155.

[35] Simon D. Round and Richard M. Duke, *"Real time optimization of an active filteres's performance"*. IEEE Trans. on Industrial Electronics, Vol. 41, No. 3, June 1994, pp. 278-284.

[36] Diego R. Veas, Juan W. Dixon and Boon-Teck Ooi, *"A novel load current control method for a leading power factor voltage source PWM rectifier"*, IEEE Trans. on Power Electronics, Vol. 9, No. 2, March 1994, pp. 153-159.

[37] Vlatko Vlatkovic and Dusan Borojevic, *"Digital-Signal-Processor-Based Control of Three-Phase Space Vector Modulated Converters"*, IEEE Trans. on Industrial Electronics, Vol. 41. No.3. June 1994, pp. 326-332.

[38] Gerard Ledwich and Parviz Doulai, *"Multiple Converter Performance and Active Filtering"*, IEEE Trans. on Power Electronics, Vol. 10, No. 3, May 1995, pp. 273-279.

[39] Y.-K.Lo, C.-L. Chen, *"Three-phase four wire voltage controlled ac line conditioner with unity input power factor and minimised output voltage harmonics"*, IEE Proc.-Electr. Power Appl., Vol. 142,N0. 1, January 1995, pp. 43-49.

[40] Luis A. Moran, Juan W. Dixon and Rogel R. Wallace, *"A three-phase active power filter operating with fixed switching frequency for reactive power and current harmonic compensation"*, IEEE Trans. on Industrial Electronics, Vol. 42, No. 4, August 1995, pp. 402-408.

[41] Nasser H. Rashidi, *"Improved and Less Load Dependent Three-Phase Current-Controlled Inverter with Hysteresis Current Controllers"*, IEEE Trans. on Industrial Electronics, Vol. 42, No. 3, June 1995, pp. 325-330.

[42] Carlo Rossi and Alberto Tonielli, *"Robust Current Controller for Three-Phase Inverter Using Finite-State Automation"*, IEEE Trans. on Industrial Electronics, Vol. 42, No. 2, April 1995, pp. 169-178.

[43] Suttichai Saetieo, Rajesh Devaraj and David A. Torrey, *"The design and implementation of a three-phase active power filter based on sliding mode control"*,, IEEE Trans. on Industry Application, Vol. 31, N0. 5, Sep/Oct 1995, pp. 993-999.

[44] David A. Torrey and Adel M. A. M. Al-Zamel, *"Single-phase active power filters for multiple nonlinear loads"*. IEEE Trans. on Power Electronics. Vol. 10, No. 3. May 1995, pp. 263-271.

[45] Navid R. Zargari and Geza Joos, *"Performance Investigation of a Current- Controlled Voltage-Regulated PWM Rectifier in Rotating and Stationary Frames"*, IEEE Trans. on Industrial Electronics, Vol. 42, No. 4, August 1995. pp.396-401.

[46] *"PSCAD/EMTDC^{TM} , Power Systems Simulation Software"*. Manitoba HVDC Research Centre, 400 – 1619 Pembina Highway, Winnipeg, Manitoba, Canada, R3T 2G5.

121283

EE-1996-M-.SUN-ACT

A121283